Electronic Supporting Information for

Shining Light on Fluoride Detection: A Comprehensive Study Exploring the Potential of Coumarin Precursors as Selective Turn-On Fluorescent Chemosensors

Sara Amer,[a] Vincent Joseph,[a] Bat-El Oded, Vered Marks, Flavio Grynszpan, and Mindy Levine**

TABLE OF CONTENTS

MATERIALS AND METHODS

Materials:

- All reagents were purchased from commercial sources and were used without further purification. All organic solvents used were HPLC grade and were dried over activated molecular sieves (3 Å or 4 Å) prior to use. NMR spectroscopy solvents were purchased from commercial sources and dried over activated molecular sieves (3 Å or 4 Å) prior to use. Ultra-pure water was obtained using a Milli-Q® machine, in which water is processed through the QPAK® purification cartridge to reach a resistivity of 18.2 MΩ•cm (25°C) and a TOC value below 5 ppb.

Methods:

- NMR spectra (^{1}H, ^{13}C) were recorded using a Bruker Avance-III 400 MHz spectrometer equipped with a 5 mm BBFO SmartProbe. All NMR spectra were processed with MestReNova v.6.0.2-5457 software (available from Mestrelab Research).
- Liquid chromatography - mass spectrometry (LC-MS) experiments were performed using an Agilent Technologies 6120 Quadrupole LC/MS. The mobile phase A was 0.1% formic acid in water, and the mobile phase B was 100% acetonitrile. The flow rate was set to 0.03 mL/min, and the run time was set to 23 minutes.
- Mixtures of products were separated and analyzed using thin layer chromatography (TLC), column chromatography, and/or medium-pressure flash chromatography with 60 mesh silica gel.
- UV-vis absorbance spectra were measured with a Varian Cary 100 Bio UV-Vis spectrophotometer, using a 10 mm path-length quartz cuvette and a scan rate of 600 nm/min. Experiments at 40 °C were monitored using an 18-cell holder transporter (model number: water-thermo 02-101628-00), made in Australia by Varian Australia Pty Ltd Non-Patient Equipment.
- Room temperature fluorescence spectra were recorded on a Varian Cary Eclipse fluorescence spectrophotometer, using a 2.5 nm excitation slit width, a 2.5 nm emission slit width, a 600 nm/min scan rate, and a 10 mm path-length quartz cuvette. Elevated temperature (40 °C) fluorescence spectra were recorded on a Jasco Spectrofluorometer FP-8500 fluorimeter, using a 2.5 nm excitation slit width, a 2.5 nm emission slit width, a 600 nm/min scan rate, and a 10 mm path-length quartz cuvette. The temperature was controlled using a Peltier-Thermo Cell Holder (model number: ETC-815/B023661516).
- Computational experiments were conducted using DFT calculations with a g16 program. The functional used in this study was BPE0. The calculations were done with a 6-311++G ** basis set, which is a triple zeta all-electron basis set that includes polarization and diffuse functions. Empirical dispersion was also used. An SMD solvation model was used to include the implicit solvation effects of acetonitrile (ε = 35.688).

EXPERIMENTAL PROCEDURES

SYNTHETIC PROCEDURES

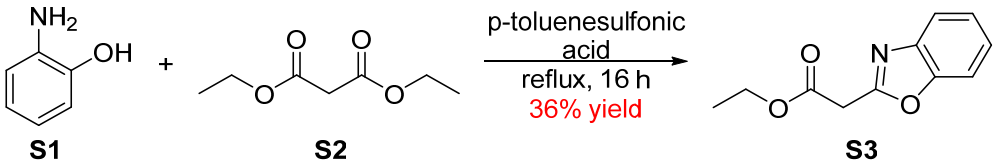

S1 **S2** **S3**

Scheme S1. Synthesis of compound **S3**

Compound S3. In a 100 mL round-bottomed flask, 2-aminophenol **S1** (1.0 g, 9.0 mmol, 1.0 equiv.) was mixed with diethyl malonate **S2** (4.32 g, 15.0 mmol, 15.0 equiv.), and *p*-toluenesulfonic acid (1.55 g, 9.0 mmol, 1.0 equiv.). The reaction mixture was flushed with nitrogen gas for 15 minutes, followed by refluxing overnight under an inert (i.e., nitrogen) atmosphere. After 16 hours, the reaction mixture was cooled to room temperature, and the solvent was evaporated under reduced pressure. The crude product was purified by column chromatography, using a solvent gradient from 20% ethyl acetate – 80% hexanes to 50% ethyl acetate- 50% hexanes. Compound **S3** was obtained as a yellow oil (674 mg, 36% yield). ^{1}H NMR spectrum (400 MHz, $CDCl_3$): δ = 7.69-7.65 (m, 1 H), 7.49-7.44 (m, 1 H), 7.29-7.25 (m, 2 H), 4.18 (q, 2 H, *J* = 7.0 Hz), 3.97 (s, 2 H), 1.22 (t, 3 H, *J* = 7.0 Hz) ppm. ^{13}C NMR spectrum (100 MHz, $CDCl_3$): δ = 166.9, 159.5, 151.0, 141.3, 125.0, 124.3, 119.6, 110.3, 61.8, 35.2, 14.2 ppm. LC-MS: $C_{11}H_{11}NO_3$, calculated: 205.07, found: 206.1 ($M + H^+$).

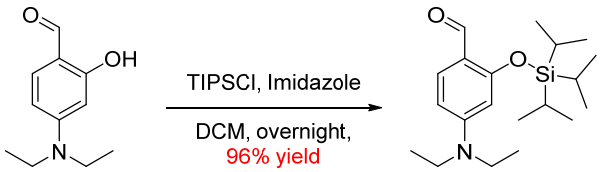

S4 **S5**

Scheme S2. Synthesis of compound **S5**

Compound S5. In a 100 mL round-bottomed flask, compound **S4** (1.0 g, 5.0 mmol, 1.0 equiv.) was dissolved in 20 mL dichloromethane. To this solution, triisopropylsilyl chloride (TIPSCl) (1.19 g, 6.0 mmol, 1.2 equiv.) and imidazole (70 mg, 10.0 mmol, 2.0 equiv.) were added. The reaction mixture was stirred at room temperature overnight, until the complete disappearance of the starting material was observed by TLC. After the reaction was complete, 10 mL of water were added, and the organic and aqueous layers were separated. The organic layer was dried over anhydrous magnesium sulfate and concentrated under reduced pressure. The crude product was purified by column chromatography, using a solvent gradient from 5% ethyl acetate – 95% hexanes to 10% ethyl acetate – 90% hexanes. Compound **S5** was obtained as a pale-yellow oil (1.73 g, 96% yield). ^{1}H NMR spectrum (400 MHz, $CDCl_3$): δ = 10.21 (d, 1 H, *J* = 0.6 Hz), 7.68 (d, 1 H, *J* = 9.0 Hz), 6.28 (ddd, 1 H, *J* = 9.0 Hz, *J* = 2.4 Hz, *J* = 0.6 Hz), 5.98 (d, 1 H, *J* = 2.4 Hz), 3.35 (q, 4 H, *J* = 7.0 Hz), 1.3 (septet, 3 H, *J* = 7.3 Hz), 1.18 (t, 6 H, *J* = 7.0 Hz), 1.13 (d, 18 H, *J* = 7.3 Hz) ppm. ^{13}C NMR spectrum (100 MHz, $CDCl_3$): δ = 187.7, 161.7, 153.8, 130.0, 116.2, 105.4, 100.1, 44.9, 18.0, 17.8, 13.2 ppm. LC-MS: $C_{20}H_{35}NO_2Si$, calculated: 349.24, found: 350.2 ($M + H^+$).

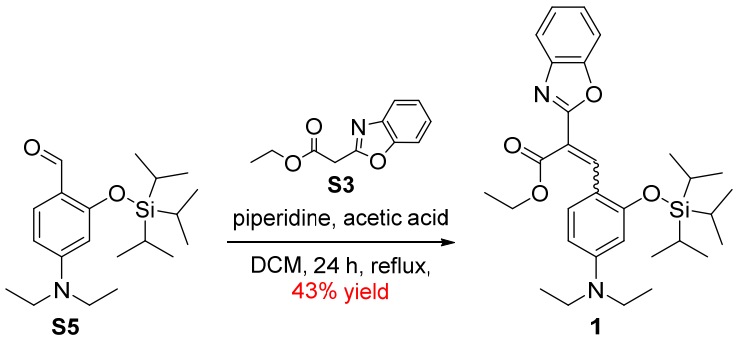

Scheme S3. Synthesis of compound **1**

Compound 1. In a 50 mL round-bottomed flask, compound **S5** (1.0 g, 2.8 mmol, 1.0 equiv.) was dissolved in anhydrous dichloromethane. To this solution were added compound **S3** (1.17 g, 5.6 mmol, 2.0 equiv.), piperidine (97 mg, 1.12 mmol, 0.4 equiv.), and acetic acid (69 mg, 1.12 mmol, 0.4 equiv.). The reaction mixture was heated at reflux overnight, followed by cooling to room temperature and removal of the solvent under reduced pressure. The crude reaction product was purified by column chromatography, using a mobile phase of 5% ethyl acetate – 95% hexanes. Compound **1** was obtained as a dark orange oil as a mixture of *Z* and *E* isomers (660 mg, 43% yield, ~ 2:1 *E*:*Z* mixture). HRMS: $C_{31}H_{44}N_2O_4Si$, calculated: 536.3070, found: 537.3149 ($M + H^+$).

Z-isomer: ^{1}H NMR spectrum (400 MHz, CD_3CN): δ = 8.25 (s, 1 H), 7.66-7.60 (m, 1 H), 7.54-7.50 (m, 1 H), 7.36-7.31 (m, 2 H), 7.29 (d, 1 H, *J* = 9.0 Hz), 6.39 (dd, 1 H, *J* = 9.0 Hz, *J* = 2.6 Hz), 6.16 (d, 1 H, *J* = 2.6 Hz), 4.39 (q, 2 H, *J* = 7.1 Hz), 3.38 (q, 4 H, *J* = 7.1 Hz), 1.44-1.37 (m, 3 H), 1.32 (t, 3 H, *J* = 7.1 Hz), 1.17 (d, 18 H, *J* = 7.1 Hz), 1.15 (t, 6 H, *J* = 7.1 Hz) ppm. ^{13}C NMR spectrum (100 MHz, CD_3CN): δ = 168.2, 163.4, 158.4, 152.2, 151.2, 142.4, 133.7, 130.5, 126.0, 120.1, 111.6, 106.8, 101.8, 62.6, 45.4, 18.4, 14.4, 12.9 ppm.

E-isomer: ^{1}H NMR spectrum (400 MHz, CD_3CN): δ =8.60 (s, 1 H), 7.78-7.74 (m, 1 H), 7.66-7.60 (m, 1 H), 7.47-7.39 (m, 2 H), 6.40 (d, 1 H, *J* = 9.1 Hz), 6.09 (d, 1 H, *J* = 2.6 Hz), 5.98 (dd, 1 H, *J* = 9.1 Hz, *J* = 2.6 Hz), 4.21 (q, 2 H, *J* = 7.1 Hz), 3.28 (q, 4 H, *J* = 7.1 Hz), 1.44-1.37 (m, 3 H), 1.22 (t, 3 H, *J* = 7.1 Hz), 1.17 (d, 18 H, *J* = 7.1 Hz), 1.06 (t, 6 H, *J* = 7.1 Hz). ^{13}C NMR spectrum (100 MHz, CD_3CN): δ = 166.8, 161.9, 159.5, 152.8, 151.6, 143.6, 142.5, 131.1, 126.0, 125.7, 121.0, 111.8, 111.0, 106.7, 101.3, 61.9, 45.3, 18.4, 18.0, 14.7, 12.8 ppm.

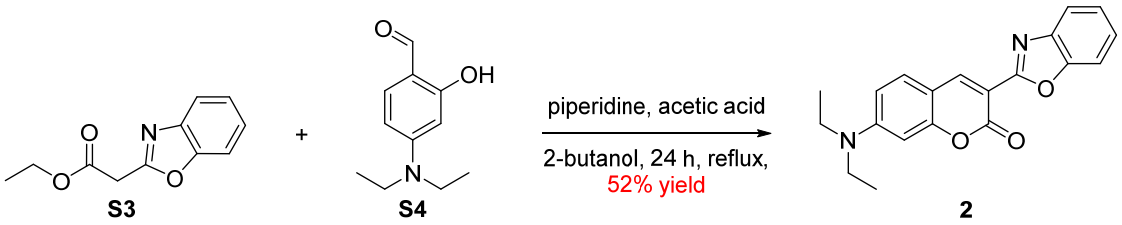

Scheme S4. Synthesis of compound **2**

Compound 2: In a 25 mL round-bottomed flask, compound **S4** (270 mg, 1.3 mmol, 1.0 equiv.) was dissolved in 10 mL of 2-butanol. Compound **S3** (230 mg, 2.0 mmol, 1.5 equiv.) was added to this solution, followed by piperidine (47 mg, 0.5 mmol, 0.4 equiv.) and acetic acid (33 mg, 0.5 mmol, 0.4 equiv.). The reaction mixture was refluxed for 24 hours. After 24 hours, the reaction mixture was cooled to room temperature, and the precipitate that formed was filtered via vacuum filtration, washed three times with 2-

butanol, and dried to give compound **2** as a pale-orange solid (242 mg, 52% yield). ^{1}H NMR spectrum (400 MHz, $CDCl_3$): δ = 8.60 (s, 1 H),7.82-7.77 (m, 1 H), 7.60-7.56 (m, 1 H), 7.41 (d, *J* = 9.0 Hz 1 H), 7.35-7.33 (m, 2H), 6.64 (dd, 1 H, *J* = 9.0 Hz, *J* = 2.5 Hz), 6.53 (d, 1 H, *J* = 2.5 Hz), 3.45 (q, *J* = 7.1 Hz 4 H), 1.25 (t, *J* = 7.1 Hz 6 H) ppm. ^{13}C NMR spectrum (100 MHz, $CDCl_3$): δ = 160.0, 158.2, 158.0, 152.1, 150.5, 145.0, 142.2, 130.7, 124.9, 124.6, 120.2, 110.4, 109.9, 108.4, 106.7, 97.1, 45.3, 12.6 ppm. HRMS: $C_{20}H_{18}N_2O_3$, calculated: 334.1317, found: 335.1396 ($M + H^+$).

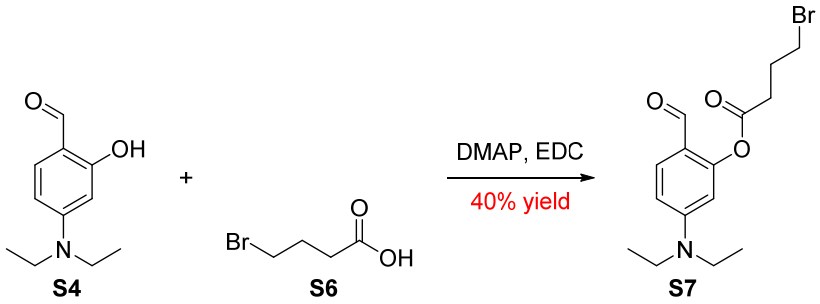

Scheme S5. Synthesis of compound **S7**

Compound S7. Compound **S4** (1.0 g, 5.0 mmol, 1.0 equiv.) was added to a round-bottomed flask. The flask was flushed with nitrogen gas for 15 minutes, followed by the addition of anhydrous acetonitrile (20 mL), compound **S6** (860 mg, 5.0 mmol, 1.0 equiv.), 4-dimethylaminopyridine (DMAP) (630 mg, 1.0 mmol, 0.2 equiv.), and 1-ethyl-3-(3-dimethylaminopropyl)carbodiimide (EDC) (1.2 g, 7.5 mmol, 1.5 equiv.). The reaction mixture was stirred at room temperature for 24 hours, while monitoring the reaction progress by thin layer chromatography. After 24 hours, the solvent was removed under reduced pressure, and the crude product was purified via column chromatography, using a solvent gradient from 10% ethyl acetate – 90% hexanes to 30% ethyl acetate – 70% hexanes. Compound **S7** was obtained as a yellow oil (699 mg, 40% yield). ^{1}H NMR spectrum (400 MHz, $CDCl_3$): δ = 9.70 (s, 1 H), 7.62 (t, 1 H, *J* = 8.9 Hz), 6.55 (dd, 1 H, *J* = 8.9 Hz, *J* = 2.5 Hz), 6.26 (d, 1 H, *J* = 8.9 Hz, 3.58 (t, 2 H, *J* = 6.4 Hz), 3.41 (q, 4 H, *J* = 7.1 Hz), 2.86 (t, 2 H, *J* = 7.1 Hz), 2.34 (tt, 2 H, *J* = 7.1 Hz, *J* = 6.4 Hz)), 1.21 (t, 6 H, *J* = 7.1 Hz) ppm. ^{13}C NMR spectrum (100 MHz, $CDCl_3$): δ = 186.9, 171.2, 168.9, 153.3, 135.0, 116.3, 108.5, 104.7, 44.9, 32.9, 32.6, 27.7, 12.7 ppm. LC-MS: $C_{15}H_{20}BrNO_3$, calculated: 341.06, found: 344.1 ($M + 3H^+$).

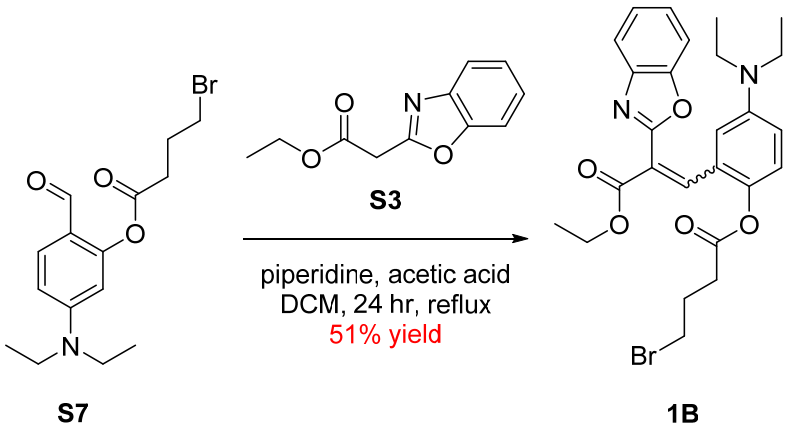

Scheme S6. Synthesis of compound **1B**

Compound 1B. In a 50 mL round-bottomed flask, compound **S7** (699 mg, 2.0 mol, 1.0 equiv.) was dissolved in 10 mL of anhydrous dichloromethane (DCM). To this solution was added compound **S3** (837

mg, 4.0 mmol, 2.0 equiv.), piperidine (69 mg, 0.81 mmol, 0.4 equiv.), and acetic acid (49 mg, 0.81 mmol, 0.4 equiv.). The reaction mixture was refluxed for overnight, followed by cooling the reaction mixture to room temperature and removal of the solvent under reduced pressure. The crude product was purified by preparative HPLC using a 70% acetonitrile – 30% water solvent mixture. Compound **1B** was obtained as a reddish-orange oil as a mixture of *Z* and *E* isomers (550 mg, 51% yield, ~ 2:1 *E*: *Z* mixture). HRMS: $C_{26}H_{29}BrN_2O_5$, calculated: 529.4228, found: 531.1322 ($M + 2H^+$).

Z-isomer: ^{1}H NMR spectrum (400 MHz, CD_3CN): δ = 7.68 (s, 1 H), 7.66-7.59 (m, 2 H), 7.41-7.36 (m, 3 H), 6.66 (dd, 1 H, *J* = 9.0 Hz, *J* = 2.6 Hz), 6.48 (d, 1 H, *J* = 2.6 Hz), 4.42 (q, 2 H, *J* = 7.1 Hz), 3.61 (t, 2 H, *J* = 6.6 Hz), 3.42 (q, 4 H, *J* = 7.1 Hz), 2.85 (t, 2 H, *J* = 7.1 Hz), 2.34-2.25 (m, 2 H), 1.34 (t, 3 H, *J* = 7.1 Hz), 1.17 (t, 6 H, *J* = 7.1 Hz) ppm. ^{13}C NMR spectrum (100 MHz, CD_3CN): δ = 172.1, 167.5, 162.4, 152.8, 152.7, 151.1, 143.0, 132.0, 130.5, 125.6, 126.9, 120.5, 118.5, 112.2, 111.4, 110.5, 105.7, 62.8, 45.3, 34.0, 34.0, 28.7, 14.4, 12.8 ppm.

E-isomer: ^{1}H NMR spectrum (400 MHz, CD_3CN): δ = 8.04 (s, 1 H), 7.80-7.75 (m, 1 H), 7.68-7.64 (m, 1 H), H), 7.49-7.42(m, 2 H), 6.64 (d, 1 H, *J* = 9.1 Hz), 6.40 (d, 1 H, *J* = 2.6 Hz), 6.27 (dd, 1 H, *J* = 9.1 Hz, *J* = 2.6 Hz), 4.24(q, 2 H, *J* = 7.1 Hz), 3.61 (t, 2 H, *J* = 6.6 Hz), 3.33 (q, 4 H, *J* = 7.1 Hz), 2.80 (t, 2 H, *J* = 7.1 Hz), 2.34-2.25 (m, 2 H), 1.24 (t, 3 H, *J* = 7.1 Hz), 1.08 (t, 6 H, *J* = 7.1 Hz) ppm. ^{13}C NMR spectrum (100 MHz, CD_3CN): δ = 172.1, 166.3, 160.9, 153.7, 152.2, 151.6, 142.2, 142.0, 131.2, 126.7, 125.7, 121.1, 115.2, 111.4, 110.7, 110.3, 105.7, 62.3, 45.3, 34.0, 33.3, 28.7, 14.6, 12.7 ppm.

PHOTOPHYSICAL EXPERIMENTAL PROCEDURES

Quantum yield experiments

The quantum yield of compound **2** was calculated using the single point relative quantum yield method, according to Equation S1:[1]

$$\phi_{F(x)} = (\frac{n_x}{n_s})^2(\frac{A_s}{A_x})(\frac{I_{f(x)}}{I_{f(s)}})\phi_{F(s)} \quad \text{(Eq. S1)}$$

where ϕ_F is the fluorescence quantum yield, A is the absorbance, I_f is the integration of the fluorescence band, and *n* is the solvent refractive index. The subscripts *s* and *x* refer to the standard and unknown samples, respectively. In this work, the fluorescence quantum yield standards were solutions of 5-30 μM of Rhodamine B in methanol.[2] To ensure the accuracy of the quantum yield of Rhodamine B, we compared its fluorescence emission to the emission of a standard solution of POPOP in ethanol.[2]

Molar absorptivity experiments

For the calculation of molar extinction coefficient, we used the Beer-Lambert equation (Eq. S2):

$$A = \varepsilon * c * l \quad \text{(Eq. S2)}$$

where *A* represents the absorbance of the sample (measured at 440 nm for compound **2**), ε represents the molar extinction coefficient, c represents the sample concentration (in mol/L), and *l* represents the path length (in cm). To do this experiment, we measured the absorbance of solutions of compound **2** at 440 nm with concentrations from 1- 4 μM. This experiment was repeated in three independent trials, and the results reported herein represent an average of the obtained results.

Selectivity experiments

A stock solution of compound **1** in acetonitrile ([**1**] = 4 μM) was divided into seven vials. To six of the vials was added 1.0 equivalent of an analyte in water ([analyte] = 4 μM; analyte = tetrabutylammonium fluoride (TBAF), tetrabutylammonium chloride (TBACl), tetrabutylammonium bromide (TBABr), tetrabutylammonium hydroxide (TBAOH), tetrabutylammonium nitrate ($TBANO_3$) or tetrabutylammonium acetate (TBAOAc)). The solution was mixed for three hours, and the steady-state UV-visible absorbance and fluorescence emission spectra (λ_{ex} = 438 nm) were recorded. This experiment was repeated in three independent trials, and the results reported herein represent an average of the obtained results.

Competition experiments

A stock solution of compound **1** in acetonitrile ([**1**] = 4 μM) was divided into six vials, and 1.0 equiv. of analyte (TBAF, TBACl, TBABr, TBAOH, $TBANO_3$, or TBAOAc) in water ([analyte] = 4 μM) was added. To the vials which did not contain TBAF, 1.0 equiv. of TBAF ([TBAF] = 4 μM) was then added. The solution was mixed for three hours and the steady-state UV-vis absorbance and fluorescence emission spectra (λ_{ex} = 438 nm) were recorded. This experiment was repeated in three independent trials, and the results reported herein represent an average of the obtained results.

Limit of detection experiments

Limits of detection were calculated following literature-reported procedures.[3] In brief, a stock solution of compound **1** in acetonitrile ([**1**] = 4 μM) was divided into seven vials, and to each vial, a different amount of TBAF was added ([TBAF] = 0.0 μM, 1.2 μM, 1.6 μM, 2.0 μM, 2.4 μM, 3.2 μM, 4.0 μM). The solution

was incubated at room temperature for three hours, and the steady-state UV-vis absorbance and fluorescence emission spectra (λ_{ex} = 438 nm) were recorded.

A graph was plotted with the integrated emission (vs. wavenumber) on the Y-axis and concentration of the analyte (in μM) on the X-axis, and an equation for the straight line was determined. The limit of detection of the blank, defined as the average of the blank plus three times the standard deviation of the blank, was entered as the Y-value for the equation, and the equation was solved for the X-value. This value was reported as the limit of detection of fluoride. Similarly, the limit of quantification of the blank was defined as the average of the blank plus ten times the standard deviation of the blank. When this value was entered in the best-fit equation, the resulting X-value was reported as the limit of quantification for the fluoride anion. This experiment was repeated in three independent trials, and the results reported herein represent an average of the obtained results.

Kinetic experiments

A solution of compound **1** in acetonitrile ([**1**] = 2 μM or 4 μM) was prepared. To this solution was added a solution of TBAF in water ([TBAF] = 4 μM or 8 μM). The steady-state UV-vis absorbance and fluorescence spectra were recorded as a function of time, both at room temperature and at 40 ºC. These experiments were repeated in three independent trials, and the results reported herein represent an average of the obtained results.

Real-world experiments

The ability of compound **1** to detect fluoride in commercial products was determined by testing its response to fluoridated mouthwash and fluoride-containing toothpaste. 3 mL of a solution of compound **1** ([**1**] = 4 μM in acetonitrile) was mixed with 10 μL of a commercial product (either 10 μL of mouthwash, or 10 μL of a solution of toothpaste, formed from mixing 10 mg of toothpaste in 1 mL of water). As a negative control, a solution of compound **1** in acetonitrile without the addition of any commercial product was tested simultaneously. The fluorescence emission spectrum of each solution was recorded from excitation at 438 nm, with the emission scanned between 440 and 600 nm (slit widths of 2.5 nm for both the excitation and emission slits). The resulting fluorescence spectra were integrated using OriginPro software, and the results obtained were compared with the reported fluoride concentrations in these products.

NMR SPECTROSCOPY EXPERIMENTAL PROCEDURES

NMR Spectra Acquisition

A sample of compound **1** (10 mg) in deuterated acetonitrile (0.6 mL) was prepared. This sample was used to acquire one-dimensional ^{1}H NMR and ^{13}C NMR spectra, as well as two-dimensional NMR spectra.

A sample of compound **2** (6.2 mg) in deuterated chloroform (0.6 mL) was prepared. This sample was used to acquire a one-dimensional ^{1}H NMR spectrum.

NMR Spectral Titrations

A sample of compound **1** (10 mg) for ^{1}H NMR spectral acquisition in deuterated chloroform (0.6 mL) was prepared, and its one-dimensional ^{1}H NMR spectrum was acquired. To this sample were added, sequentially, 0.33 equiv. of TBAF (0.01 μM) and 1.0 equiv. of TBAF (0.03 μM) in D_2O. Following each addition, the one-dimensional ^{1}H NMR spectrum was acquired.

HPLC EXPERIMENTAL PROCEDURES

An analogue of compound **1** (compound **1B**) was prepared, and the two alkene isomers were separated by preparative HPLC using a solvent gradient of 30% water-70% acetonitrile to 0% water – 100% acetonitrile over 16 minutes.

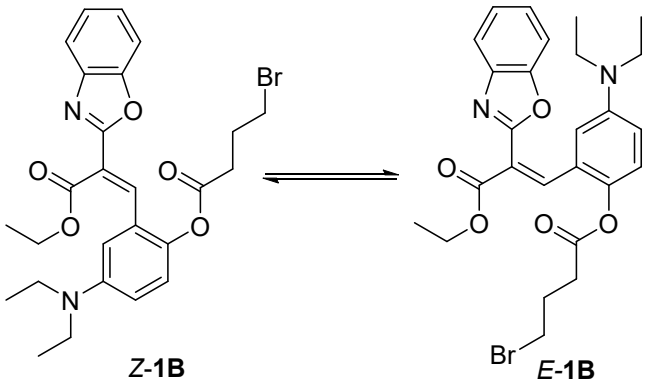

Scheme S7. Equilibration of the (*E*)- and (*Z*-) isomers of compound **1B**

SUMMARY TABLES

QUANTUM YIELD AND MOLAR ABSORPTIVITY STUDIES

Table S1. Photophysical parameters of solutions of compound **2** in acetonitrile[a]

Photophysical parameter	Calculated value	Literature-reported values[4]
Relative quantum yield (Φ)	78 ± 2%	0.80
Molar absorptivity coefficient (ε)	50,276 ± 315 M^{-1} cm^{-1}	45,709 M^{-1} cm^{-1}

[a] Relative quantum yield and molar absorptivity coefficient were determined following the procedures detailed above (*vide supra*), and the results were compared with literature-reported values.

SELECTIVITY STUDIES

Table S2. Fluorescence emission of acetonitrile solutions of compound **1** [4 μM] after exposure to various analytes[a]

Analyte	Normalized integrated emission	Normalized fluorescence intensity (at 488 nm)
none	0.001 ± 0.000	0.001 ± 0.000
TBAF	0.978 ± 0.038	0.980 ± 0.035
TBACl	0.001 ± 0.000	0.001 ± 0.000
TBABr	0.001 ± 0.000	0.001 ± 0.000
TBAOH	0.004 ± 0.002	0.004 ± 0.002
$TBANO_3$	0.002 ± 0.000	0.002 ± 0.000
TBAOAc	0.015 ± 0.005	0.014 ± 0.005

[a] Normalized integration emission was determined by integrating the full spectrum fluorescence emission vs. wavenumber on the X-axis; normalized fluorescence intensity was determined by measuring the fluorescence intensity at 488 nm. All results represent an average of three independent trials.

Table S3. Quantitative analysis of the UV-vis absorbance spectra of acetonitrile solutions of compound **1** [4 μM] after exposure to various analytes[a]

Analyte	Maximum absorbance	Wavelength of maximum absorbance	Normalized integrated absorbance
none	0.127 ± 0.004	400.7 ± 0.6	0.65 ± 0.04
TBAF	0.187 ± 0.013	436.0 ± 0.1	0.95 ± 0.09
TBACl	0.128 ± 0.005	401.4 ± 0.6	0.66 ± 0.03
TBABr	0.128 ± 0.005	401.0 ± 0.0	0.66 ± 0.05
TBAOH	0.128 ± 0.002	401.4 ± 0.6	0.67 ± 0.04
$TBANO_3$	0.127 ± 0.004	401.4 ± 0.6	0.65 ± 0.05
TBAOAc	0.126 ± 0.004	401.7 ± 0.6	0.64 ± 0.04

[a] Maximum absorbance: the highest absorbance value recorded between 300 and 700 nm; wavelength of maximum absorbance: the wavelength at which the highest absorbance value was recorded; normalized integrated absorbance: the normalized integration values of the absorbance spectra between 300 and 700 nm. All results represent an average of three independent trials.

Table S4. Normalized fluorescence emission of acetonitrile solutions of compound **1** [10 μM] after exposure to various analytes[a]

Analyte	Normalized integrated emission	Normalized fluorescence intensity (at 488 nm)
none	0.00	0.00
TBAF	1.00	1.00
TBACl	0.00	0.00
TBABr	0.00	0.00
TBAOH	0.02	0.02
$TBANO_3$	0.00	0.00
TBAOAc	0.09	0.09
water	0.01	0.01

[a] Normalized integration emission was determined by integrating the full spectrum fluorescence emission vs. wavenumber on the X-axis; normalized fluorescence intensity was determined by measuring the fluorescence intensity at 488 nm.

Table S5. Quantitative analysis of the UV-vis absorbance spectra of acetonitrile solutions of compound **1** [10 μM] after exposure to various analytes[a]

Analyte	Maximum absorbance	Wavelength of maximum absorbance	Normalized integrated absorbance
none	0.31	401	0.80
TBAF	0.41	436	1.00
TBACl	0.31	401	0.81
TBABr	0.31	402	0.80
TBAOH	0.31	401	0.83
$TBANO_3$	0.31	401	0.83
TBAOAc	0.30	402	0.81
water	0.31	401	0.81

[a] Maximum absorbance: the highest absorbance value recorded between 300 and 700 nm; wavelength of maximum absorbance: the wavelength at which the highest absorbance value was recorded; normalized integrated absorbance: the normalized integration values of the absorbance spectra between 300 and 700 nm.

COMPETITION STUDIES

Table S6. Normalized fluorescence emission of acetonitrile solutions of compound **1** after exposure to various analytes and additional TBAF[a]

Analyte	Normalized integrated emission	Normalized fluorescence intensity
none	0.01 ± 0.02	0.01 ± 0.02
TBAF	0.93 ± 0.06	0.93 ± 0.05
TBAF + TBACl	0.85 ± 0.10	0.85 ± 0.10
TBAF + TBABr	0.93 ± 0.05	0.94 ± 0.05
TBAF + TBAOH	0.94 ± 0.07	0.94 ± 0.07
TBAF + $TBANO_3$	0.92 ± 0.05	0.92 ± 0.05
TBAF + TBAOAc	0.93 ± 0.03	0.93 ± 0.03

[a] [**1**] = 4 μM. Normalized integration emission was determined by integrating the full spectrum fluorescence emission vs. wavenumber on the X-axis; normalized fluorescence intensity was determined by measuring the fluorescence intensity at 488 nm.

Table S7. Quantitative analysis of the UV-vis absorbance spectra of acetonitrile solutions of compound **1** after exposure to various analytes and additional TBAF[a]

Analyte	Maximum absorbance	Wavelength of maximum absorbance	Normalized integrated absorbance
none	0.12 ± 0.00	401 ± 2	0.61 ± 0.03
TBAF	0.18 ± 0.01	437 ± 1	0.92 ± 0.03
TBAF + TBACl	0.17 ± 0.01	435 ± 3	0.86 ± 0.05
TBAF + TBABr	0.18 ± 0.01	437 ± 1	0.89 ± 0.06
TBAF + TBAOH	0.18 ± 0.01	437 ± 1	0.89 ± 0.10
TBAF + $TBANO_3$	0.18 ± 0.01	436 ± 1	0.90 ± 0.09
TBAF + TBAOAc	0.18 ± 0.01	437 ± 1	0.87 ± 0.04

[a] [**1**] = 4 μM. Maximum absorbance: the highest absorbance value recorded between 300 and 700 nm; wavelength of maximum absorbance: the wavelength at which the highest absorbance value was recorded; normalized integrated absorbance: the normalized integration values of the absorbance spectra between 300 and 700 nm.

LIMIT OF DETECTION STUDIES

Table S8. Limits of detection and quantification of fluoride anion (introduced as TBAF) based on the changes in the fluorescence emission of compound **1**[a]

Limit of detection (LOD) (M)	7.46E-9 ± 3.48E-10
Limit of quantification (LOQ) (M)	2.49E-8 ± 1.16E-9
Best linear fit equation	y = 7.0E9x + 1524
R^2 value	0.9952

[a] Limits of detection and quantification were obtained following the procedures detailed above (*vide supra*). All results represent an average of three trials.

Table S9. Literature-reported limits of detection of fluoride anion via other fluorescence and colorimetric-based sensors

Sensing compound	Solvent system	LOD (M)	Reference
Benzothiazolium hemicyanine dye	Ethanol-water	8.00×10^{-5}	*5*
Sugar-functionalized fluorescent probe	Phosphate buffer	2.00×10^{-5}	*6*
Triisopropylsilyl-substituted coumarin	Acetonitrile	$\sim 50 \times 10^{-9}$	*7*
Difluoroboradiaza-*s*-indacene coumarin	DMSO	1.20×10^{-7}	*8*
Silyl-protected methylquinoline	THF	1.00×10^{-6}	*9*
Trihexylsilylacetylene-containing BODIPY	Acetone	6.74×10^{-8}	*10*
Fe(III)-complexed thiosemicarbazone	HEPES: DMSO	1.40×10^{-4}	*11*
1,2-bis(*o*-aminophenoxy)-ethane-*N,N,N',N'*-tetraacetic acid	Water	3.00×10^{-4}	*12*
8-hydroxyquinoline–Zr(IV)–EDTA complex	Ethanol-water	6.00×10^{-7}	*13*
1,3-*alt*-thiacalix[4]arene	THF	2.60×10^{-7}	*14*
Perylenediimide derivative	Dichloromethane	1.40×10^{-4}	*15*
Indole-conjugated cyano-quinazolinone	DMSO	8.80×10^{-4}	*16*
4-Chloro-2,6-bis(hydroxymethyl)phenol	DMSO	4.00×10^{-7}	*17*
2,4,5-Triphenylpyridinium	Acetonitrile	2.70×10^{-6}	*18*
2-(4-Aminophenyl)-benzothiazole-based maleimide	DMSO	5.00×10^{-5}	*19*
4-(2-Acryloyloxyethylamino)-7-nitro-2,1,3-benzoxadiazole (NBDAE)-labeled polymers	THF	8.00×10^{-7}	*20*
Cysteamine-capped quantum dots	H_2O	5.00×10^{-6}	*21*
Anthraquinone immobilized on mesoporous silica	H_2O	5.00×10^{-7}	*22*
CdSe / ZnS quantum dots	Acetonitrile	7.40×10^{-2}	*23*
This work	Acetonitrile	7.00×10^{-9}	

REAL-WORLD SAMPLE STUDIES

Table S10. A summary of the fluorescence response of solutions of compound **1** following exposure to fluoride-containing commercial products[a]

Sample	Normalized integrated emission[b]	Fluorescence increase factor[c]	Calculated $[F^-]$[d]	Reported $[F^-]$[e]
None	0.16	1.0-fold	--	--
Mouthwash	1.00	6.3-fold	0.63 ± 0.03 ppm	0.75 ppm
Toothpaste	0.57	3.6-fold	*f*	*f*

[a] [**1**] = 4 μM in acetonitrile; $\lambda_{excitation}$ = 438 nm; $\lambda_{recorded}$ = 440-600 nm; excitation slit width = emission slit width = 2.5 nm

[b] Fluorescence spectra were integrated between 455 and 600 nm using OriginPro software, with the highest integration value normalized to 1.00.

[c] Fluorescence increase factors were calculated by dividing the integrated emission of solutions of compound **1** in the presence of fluoride-containing commercial products by the integrated emission of compound **1** in the absence of the commercial product.

[d] Calculated fluoride concentrations were determined by using a calibration curve.

[e] Reported fluoride concentrations were determined by using the fluoride concentrations values reported for each commercial product, with modifications as needed to account for the dilution of the product during the experiment.

[f] The amorphous nature of toothpaste made it difficult to quantitatively determine the fluoride concentrations.

KINETIC STUDIES

Table S11. Summary of kinetic data of the reaction between compound **1** and fluoride anion[a]

Temperature	[**1**] (μM)	[F^-] (μM)	Rate constants of first order reaction (min^{-1})
Room temperature	4	4	0.0218
Room temperature	4	8	0.0707
Room temperature	2	4	0.0235
40 °C	4	4	0.1635

[a] Fluoride was introduced as TBAF; solutions of **1** and TBAF were mixed in acetonitrile; all results were calculated from the average of three independent trials

COLORIMETRIC STUDIES

Solution-state colorimetric studies

Table S12. Quantitative colorimetric values of solutions of compound **1** after exposure to various analytes, photographed under ambient light or under 365 nm excitation[a]

	AMBIENT LIGHT		365 NM LIGHT EXCITATION	
	(R+G+B)/3	0.299R+0.587G+0.114B	(R+G+B)/3	0.299R+0.587G+0.114B
no analyte	120.2	123.7	22.7	11.7
TBAF	98.8	112.1	105.0	129.8
TBABr	92.5	94.4	14.2	7.4
TBACl	99.6	102.9	15.9	8.2
TBAOH	92.4	94.4	12.3	6.8
$TBANO_3$	92.5	94.4	10.5	5.9
TBAOAc	113.4	116.0	10.5	6.0

[a] Images were obtained from photographs of the solutions ([**1**] = 10 μM), taken either under ambient light or under excitation with a hand-held, long-wave TLC lamp (365 nm excitation), after exposure to analytes (10 μM). Quantitative colorimetric values were obtained using ImageJ software.

Solid-state colorimetric studies

Table S13. Quantitative colorimetric values of the filter papers functionalized with compound **1** after exposure to various analytes, photographed under ambient light or under 365 nm excitation[a]

	AMBIENT LIGHT		365 NM LIGHT EXCITATION	
	(R+G+B)/3	0.299R+0.587G+0.114B	(R+G+B)/3	0.299R+0.587G+0.114B
no analyte	110.6 ± 4.9	142.5 ± 7.0	12.3 ± 8.6	11.5 ± 11.2
TBAF	62.0 ± 18.0	75.3 ± 22.5	118.9 ± 4.3	148.8 ± 0.2
TBABr	106.2 ± 7.2	137.0 ± 10.4	15.9 ± 2.2	18.0 ± 1.2
TBACl	105.8 ± 0.2	136.1 ± 0.2	19.6 ± 9.2	22.6 ± 11.3
TBAOH	108.2 ± 5.3	138.9 ± 7.5	31.0 ± 18.8	37.5 ± 23.5
$TBANO_3$	102.3 ± 4.7	129.9 ± 6.5	24.6 ± 10.7	30.4 ± 13.5
TBAOAc	90.0 ± 13.1	112.3 ± 17.1	31.4 ± 18.7	38.7 ± 24.0

[a] Images were obtained from photographs of Whatman #1 filter papers, taken either under ambient light or under excitation with a hand-held, long-wave TLC lamp (365 nm excitation), after exposure to analytes (two drops of a 6 mM solution of each analyte). Quantitative colorimetric values were obtained using ImageJ software. All results represent an average of two trials.

NMR SPECTROSCOPY STUDIES

Table S14. Coupling correlations observed in the NOESY and COESY NMR spectra of compound **1**[a]

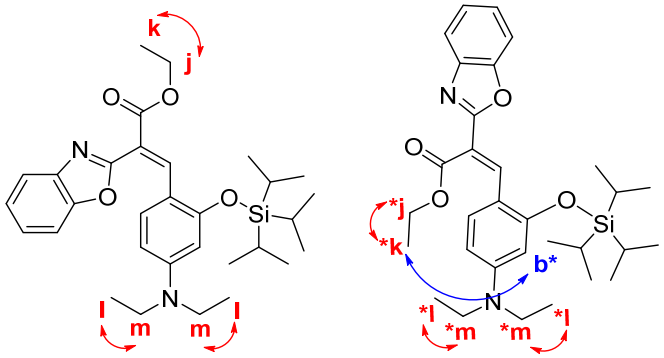

COSY		NOESY
E-isomer	*Z*-isomer	*Z*-isomer
k (1.22 ppm) – j (4.21 ppm)	*k (1.31 ppm) - *j (4.40 ppm)	*k (1.31 ppm) - *b (6.16 ppm)
l (1.05 ppm) – m (3.28 ppm)	*l (1.15 ppm) - *m (3.38 ppm)	

[a] Red arrows in the figure indicate correlations observed in the two-dimensional COSY spectra of *E*-**1** and *Z*-**1**; the blue arrow indicates the correlation observed in the NOESY spectrum of *Z*-**1**

Table S15. Chemical shifts for the ^{1}H NMR spectral titration studies of compound **1** with TBAF[a]

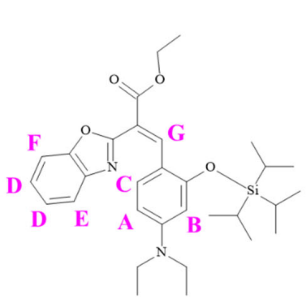

(*E*)-**1**

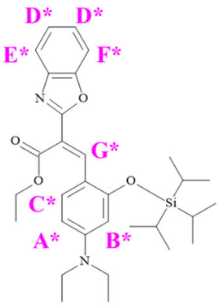

(*Z*)-**1**

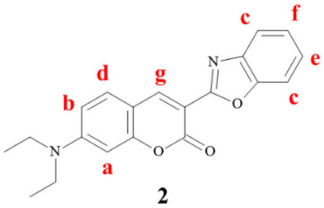

2

Compound **1** (*E*- and *Z*- isomers)	Compound **1** + 0.33 equivalents TBAF	Compound **1** + 1.0 equivalents TBAF	Compound **2**
-	6.52 (a)	6.50 (a)	6.54 (a)
-	6.64 (b)	6.62 (b)	6.64 (b)
-	7.32 (c)	7.30 (c)	7.33 (c)
-	7.41 (d)	7.38 (d)	7.41 (d)
-	7.57 (e)	7.55 (e)	7.58 (e)
-	7.79 (f)	7.76 (f)	7.79 (f)
-	8.60 (g)	8.58 (g)	8.61 (g)
5.94 (A)	5.92 (A)	-	-
6.04 (B)	6.03 (B)	-	-
6.13 (A*)	6.11 (A*)	-	-
6.25 (B*)	6.24 (B*)	-	-
6.52 (C)	6.51 (C)	-	-
8.32 (G*)	8.31 (G*)	-	-
8.67 (G)	8.65 (G)	-	-

[a] TBAF: tetra-*n*-butyl ammonium fluoride; the original sample of compound **1** was a mixture of isomers (73% *E*-1 and 27% Z-**1**); these experiments were conducted in $CDCl_3$ at room temperature

COMPUTATIONAL STUDIES

Table S16. Cartesian coordinates of the optimized structure of compound (*E*)-**1**

6	6.382142000	-1.123462000	-1.879646000
6	5.289870000	-1.031031000	-1.020810000
6	5.496707000	-0.858180000	0.350507000
6	6.743858000	-0.766820000	0.936020000
6	7.825796000	-0.864043000	0.066513000
6	7.646758000	-1.038976000	-1.312646000
7	3.927468000	-1.061589000	-1.259644000
6	3.388339000	-0.925469000	-0.087042000
8	4.275226000	-0.795463000	0.942968000
6	1.973441000	-0.951335000	0.233223000
6	1.126472000	-1.517126000	-0.657688000
6	1.551935000	-0.368849000	1.533208000
6	-0.318156000	-1.567844000	-0.648507000
8	0.574939000	-1.085646000	2.093777000
6	-0.955114000	-2.709323000	-1.153975000
6	-2.324158000	-2.859035000	-1.187898000
6	-3.163555000	-1.816391000	-0.742039000
6	-2.536426000	-0.649320000	-0.273507000
6	-1.154180000	-0.512030000	-0.236926000
8	-0.602492000	0.653846000	0.161262000
14	-1.081471000	2.219103000	-0.327914000
6	0.379451000	3.347962000	0.041480000
6	-1.503556000	2.175350000	-2.181172000
6	-2.637090000	2.716264000	0.653432000
6	1.655124000	2.900895000	-0.678008000
6	0.651598000	3.569260000	1.531710000
6	-0.683325000	1.177087000	-3.002385000
6	-1.413129000	3.574362000	-2.801929000

6	-2.655139000	2.169136000	2.082523000
6	-2.879420000	4.228789000	0.646256000
7	-4.540044000	-1.915982000	-0.789112000
6	-5.316964000	-0.830036000	-0.206994000
6	-5.143940000	-3.237306000	-0.834960000
6	-6.811257000	-0.917950000	-0.452094000
6	-5.078286000	-3.986012000	0.490296000
8	2.043381000	0.608745000	2.039410000
6	-0.031781000	-0.517697000	3.258679000
6	-1.266020000	-1.329996000	3.559008000
1	6.240995000	-1.254986000	-2.946197000
1	6.868447000	-0.627719000	2.003033000
1	8.832119000	-0.801234000	0.466079000
1	8.521414000	-1.107857000	-1.950560000
1	1.606812000	-2.001123000	-1.506681000
1	-0.333390000	-3.523636000	-1.514597000
1	-2.734326000	-3.782731000	-1.571581000
1	-3.122122000	0.184632000	0.080909000
1	0.069460000	4.313402000	-0.389208000
1	-2.554984000	1.856688000	-2.230371000
1	-3.476554000	2.258163000	0.108322000
1	2.467816000	3.610580000	-0.485714000
1	1.522816000	2.837835000	-1.761422000
1	1.985631000	1.923414000	-0.319613000
1	1.477309000	4.279074000	1.659502000
1	-0.214144000	3.980200000	2.058073000
1	0.950250000	2.640275000	2.022003000
1	-0.956676000	1.248471000	-4.061892000
1	-0.853631000	0.146172000	-2.686872000
1	0.390882000	1.369183000	-2.929753000

1	-1.753428000	3.552368000	-3.843539000
1	-2.021370000	4.315838000	-2.275879000
1	-0.381111000	3.939571000	-2.806421000
1	-3.603108000	2.412230000	2.577366000
1	-2.531727000	1.083301000	2.109650000
1	-1.853154000	2.602359000	2.686979000
1	-3.803309000	4.472843000	1.183640000
1	-2.976608000	4.630503000	-0.365936000
1	-2.065907000	4.769989000	1.138482000
1	-5.125621000	-0.749502000	0.876049000
1	-4.961665000	0.103133000	-0.654763000
1	-6.180240000	-3.124089000	-1.154734000
1	-4.664541000	-3.815302000	-1.627044000
1	-7.278271000	0.001599000	-0.090495000
1	-7.036517000	-1.010975000	-1.518124000
1	-7.280755000	-1.750259000	0.077952000
1	-5.533014000	-4.976561000	0.397988000
1	-4.041935000	-4.113188000	0.814354000
1	-5.612717000	-3.441711000	1.274874000
1	0.688650000	-0.538830000	4.081902000
1	-0.271239000	0.527637000	3.049471000
1	-1.783197000	-0.914061000	4.428037000
1	-1.949525000	-1.317846000	2.705886000
1	-1.007611000	-2.369384000	3.775812000

Table S17. Cartesian coordinates of the optimized structure of compound (*Z*)-**1**

6	-2.164633000	-1.502715000	-0.820452000
6	-1.182206000	-2.329506000	-0.395534000
6	-3.586007000	-1.902743000	-0.745820000
6	-1.873437000	-0.249889000	-1.507844000

6	0.240047000	-2.067075000	-0.360658000
7	-0.940310000	-0.037231000	-2.377178000
6	-1.058634000	1.304860000	-2.693073000
6	-2.125496000	1.838934000	-1.966719000
8	-2.647815000	0.836538000	-1.214021000
6	-0.320486000	2.122402000	-3.544185000
6	-0.688364000	3.459158000	-3.620302000
6	-1.762695000	3.970411000	-2.878936000
6	-2.513850000	3.162956000	-2.030281000
6	1.136344000	-3.076361000	-0.731003000
6	2.500660000	-2.887825000	-0.782531000
6	3.060802000	-1.643592000	-0.423608000
6	2.172072000	-0.640143000	-0.002982000
6	0.800408000	-0.846494000	0.059735000
7	4.424777000	-1.423949000	-0.447019000
6	4.896199000	-0.075296000	-0.162801000
6	5.252889000	-2.269225000	-1.291311000
6	5.116362000	-1.969712000	-2.778842000
6	6.401814000	0.054092000	-0.031134000
8	-0.007817000	0.103744000	0.571131000
14	0.331782000	1.099392000	1.911631000
6	-1.349362000	1.608228000	2.599256000
6	-2.190257000	0.398734000	3.017867000
6	-2.161803000	2.515907000	1.674617000
6	1.338883000	0.109629000	3.186961000
6	0.978962000	-1.373764000	3.296641000
6	1.281700000	0.778379000	4.565059000
6	1.357130000	2.581180000	1.305279000
6	1.059515000	2.945267000	-0.151415000
6	1.243677000	3.807835000	2.215261000

8	-4.478332000	-1.371273000	-1.360838000
8	-3.776710000	-2.944721000	0.084564000
6	-5.127026000	-3.411681000	0.210809000
6	-5.896921000	-2.591365000	1.220971000
1	-1.497244000	-3.318990000	-0.073313000
1	0.510501000	1.723567000	-4.114604000
1	-0.133395000	4.128351000	-4.269151000
1	-2.015937000	5.021191000	-2.969592000
1	-3.346749000	3.546347000	-1.453411000
1	0.732180000	-4.041331000	-1.022942000
1	3.124528000	-3.710065000	-1.103803000
1	2.537242000	0.333856000	0.287170000
1	4.530226000	0.635390000	-0.922091000
1	4.452522000	0.231958000	0.789272000
1	6.289590000	-2.150565000	-0.974494000
1	5.011867000	-3.313824000	-1.086262000
1	5.746643000	-2.642087000	-3.368155000
1	4.080974000	-2.093175000	-3.107063000
1	5.419757000	-0.942130000	-3.001133000
1	6.636350000	1.065849000	0.309219000
1	6.800332000	-0.648330000	0.706252000
1	6.925702000	-0.099089000	-0.977802000
1	-1.101799000	2.182878000	3.505111000
1	-3.169680000	0.723934000	3.387950000
1	-1.716429000	-0.182886000	3.812719000
1	-2.363351000	-0.271718000	2.170061000
1	-3.060127000	2.874780000	2.190977000
1	-1.602680000	3.392538000	1.338333000

SUMMARY FIGURES

NMR SPECTRA

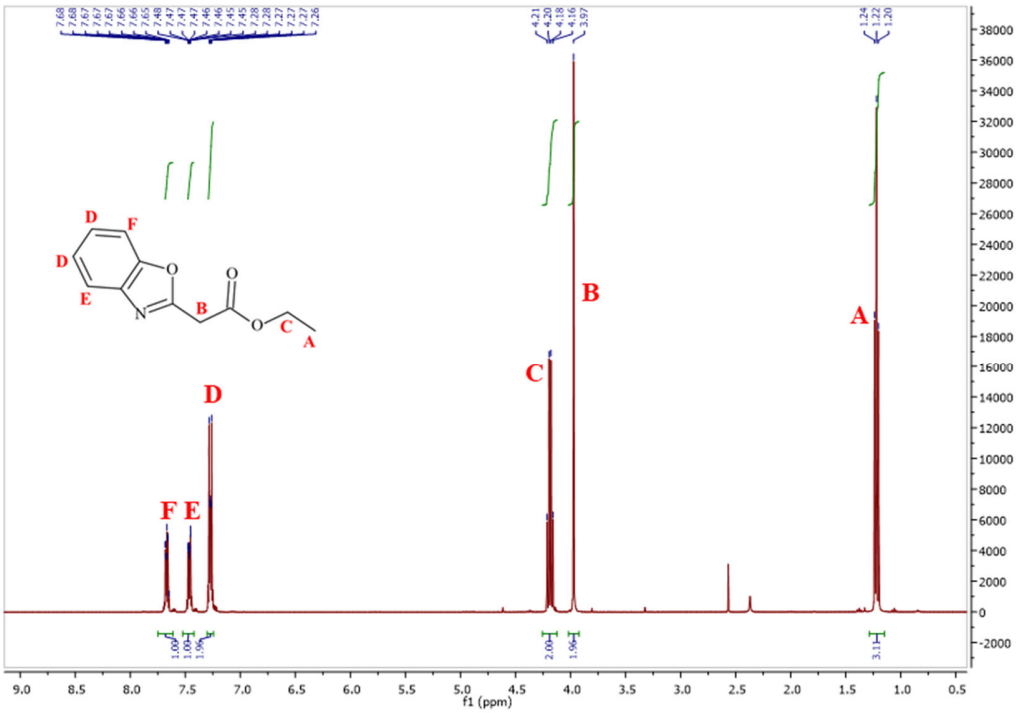

Figure S1. ^{1}H NMR spectrum of compound **S3**

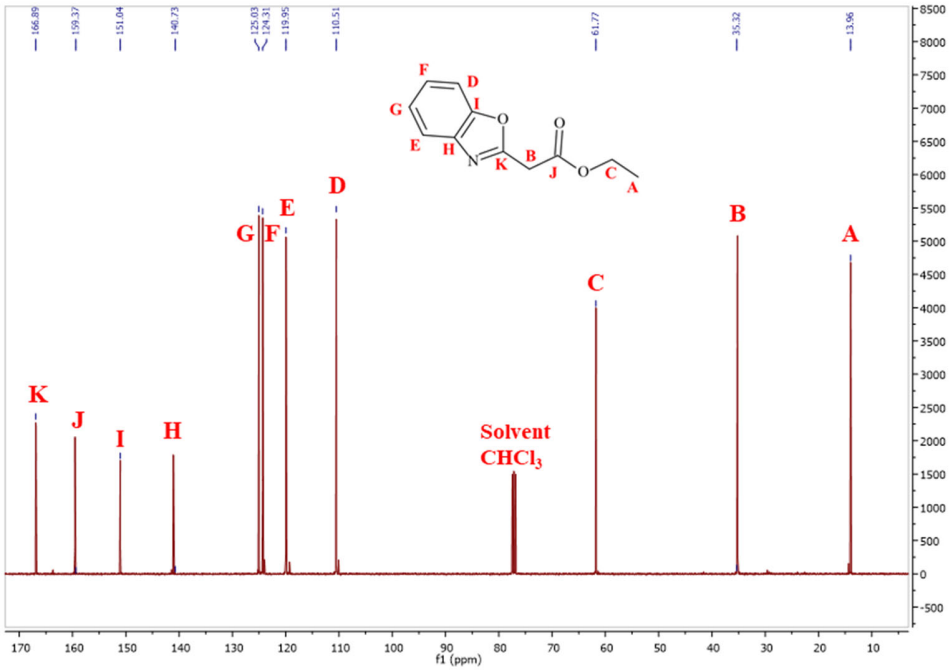

Figure S2. ^{13}C NMR spectrum of compound **S3**

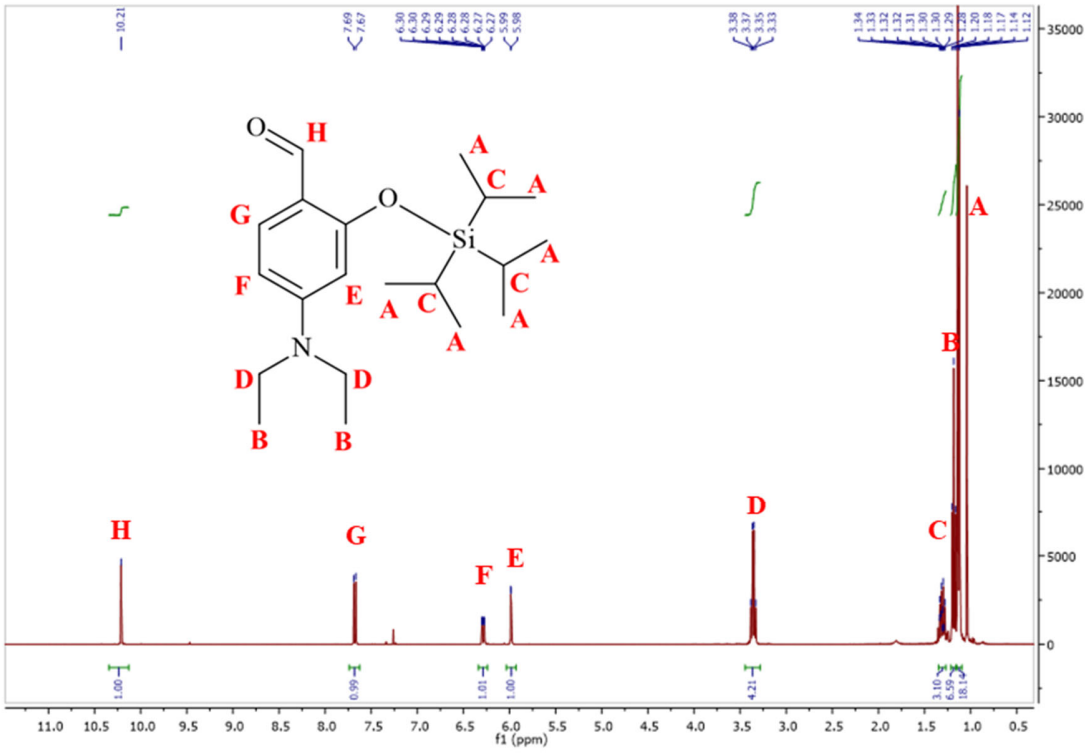

Figure S3. [1]H NMR spectrum of compound **S5**

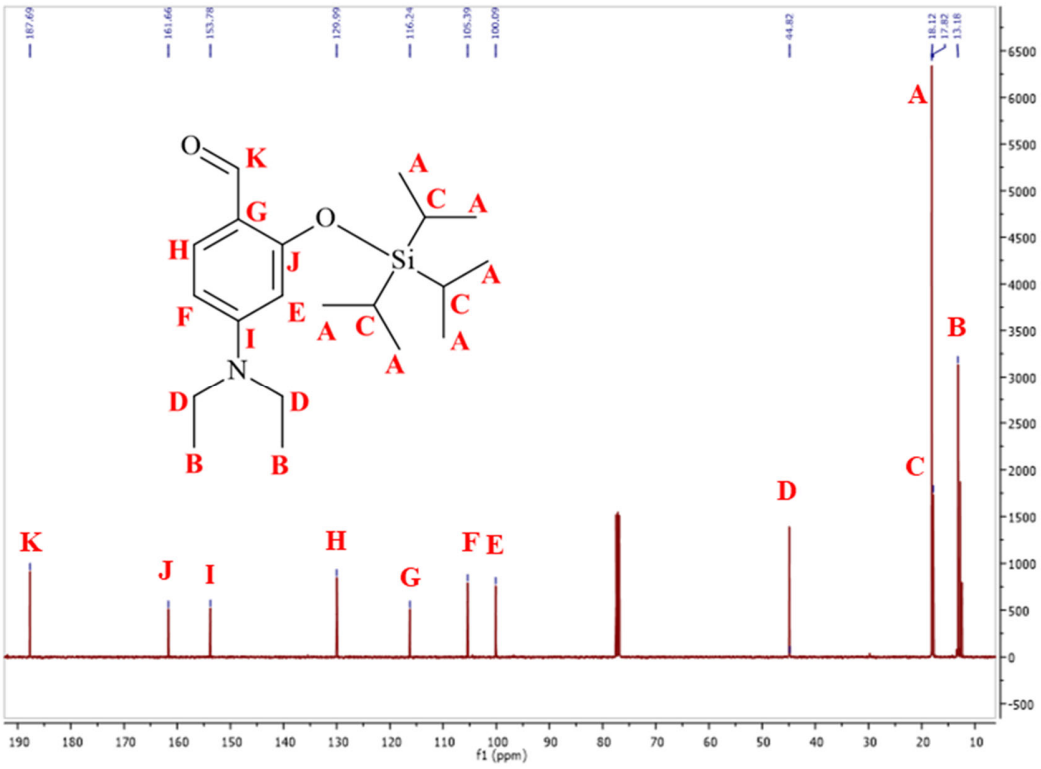

Figure S4. [13]C NMR spectrum of compound **S5**

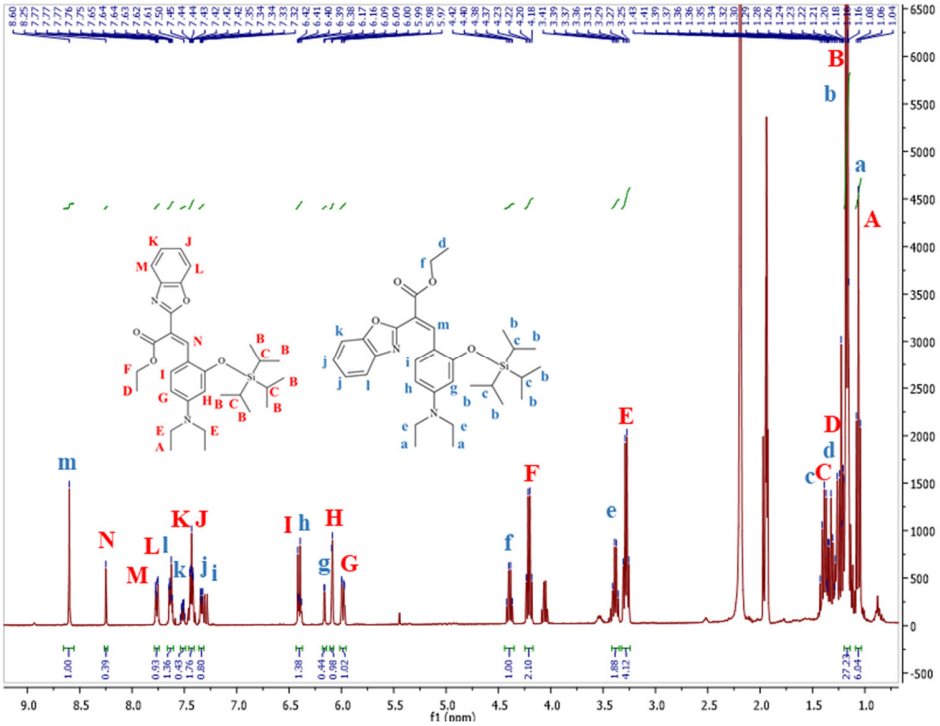

Figure S5. ^{1}H NMR spectrum of compound **1** (mixture of *Z* and *E* isomers) in CD_3CN

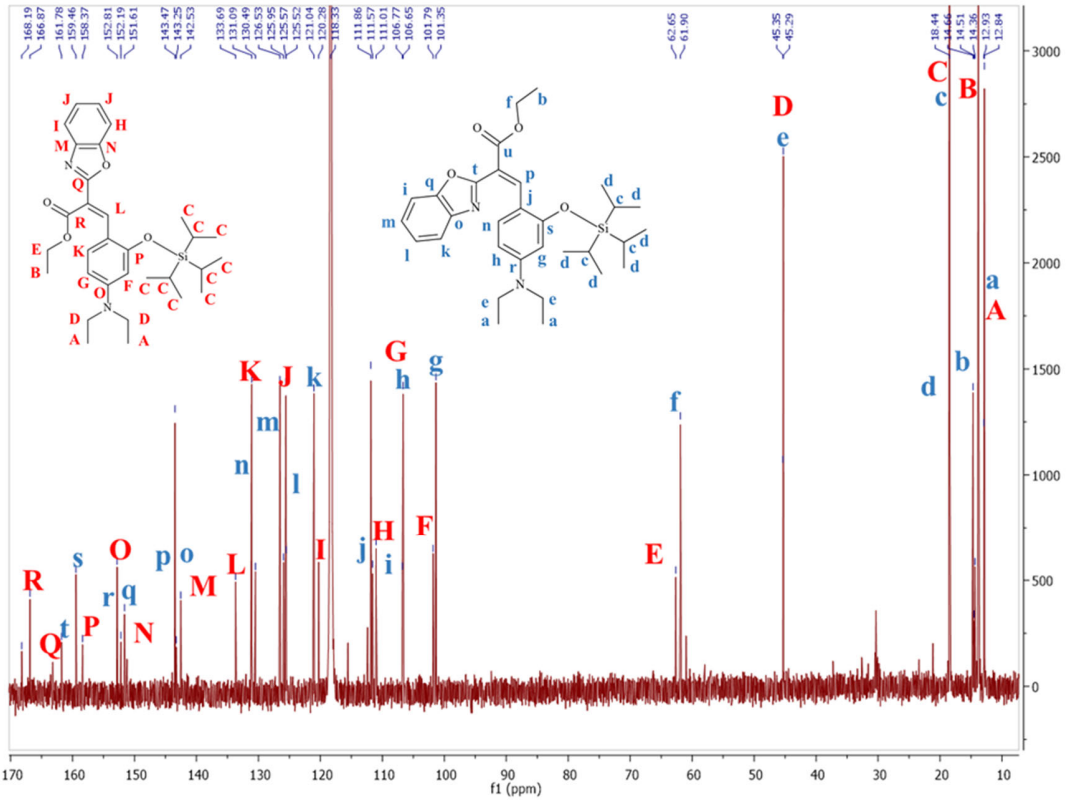

Figure S6. ^{13}C NMR spectrum of compound **1** (mixture of *Z* and *E* isomers) in CD_3CN

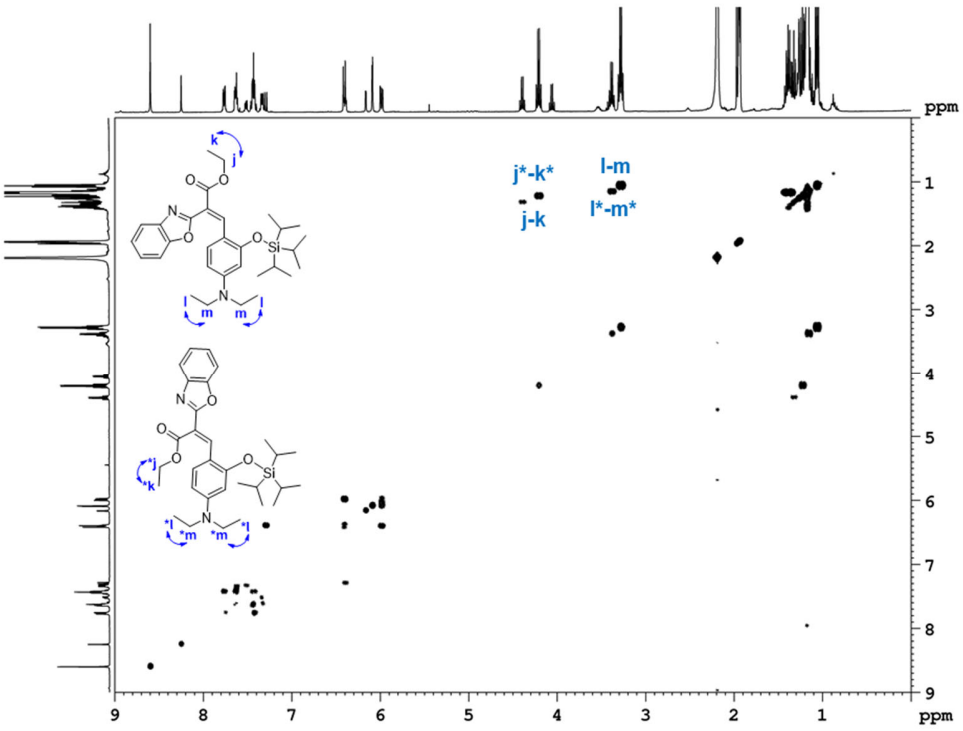

Figure S7. COSY NMR spectrum of compound **1** (mixture of *Z* and *E* isomers) in CD_3CN

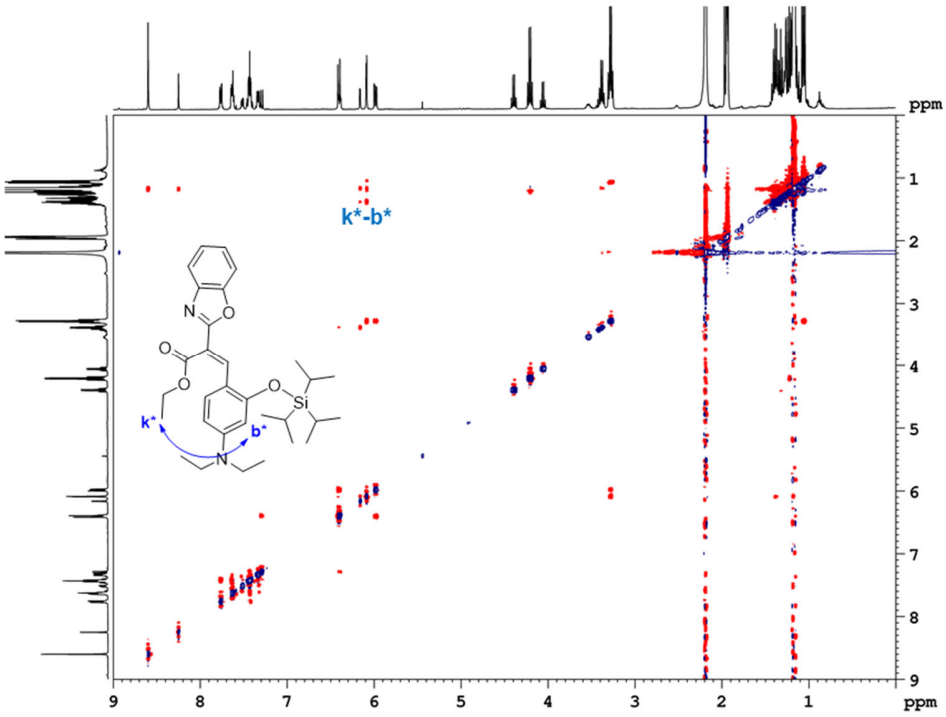

Figure S8. NOESY NMR spectrum of compound **1** (mixture of *Z* and *E* isomers) in CD_3CN

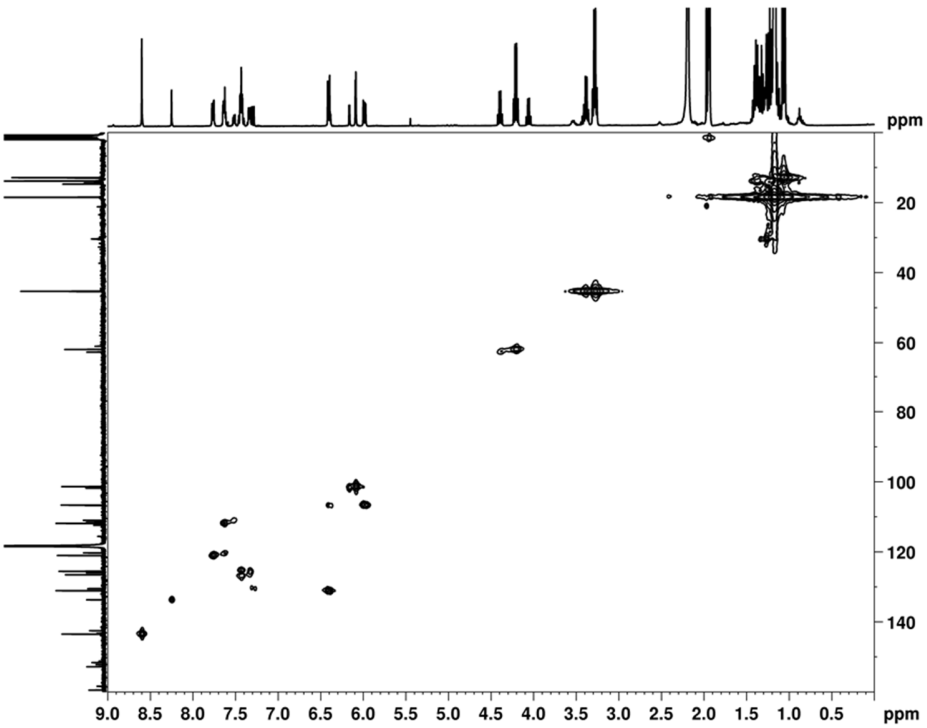

Figure S9. HMQC NMR spectrum of compound **1** (mixture of *Z* and *E* isomers) in CD_3CN

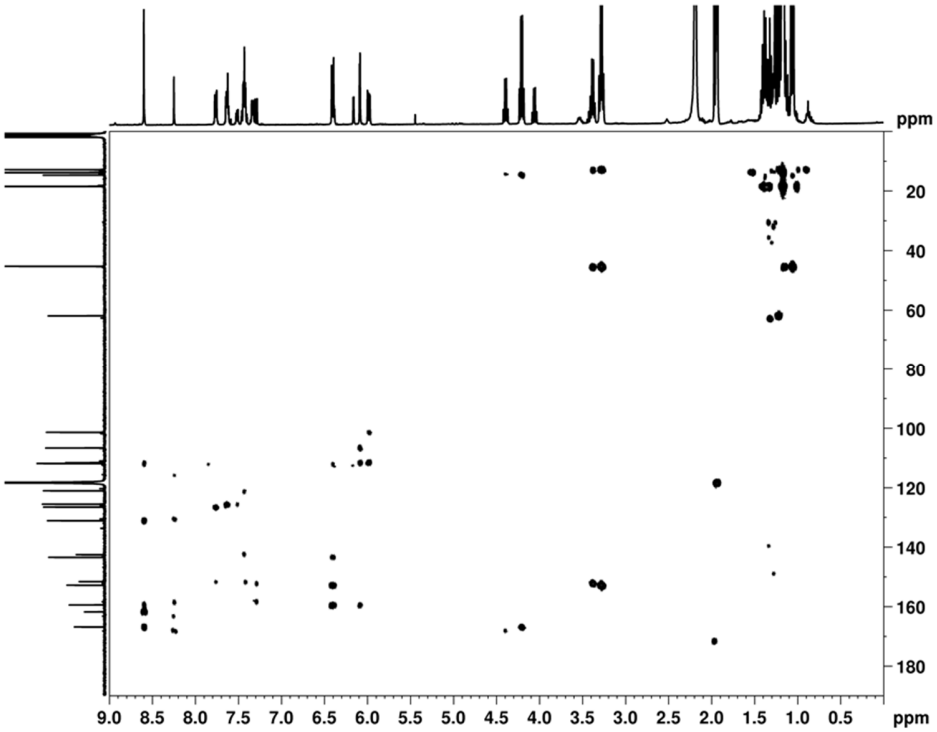

Figure S10. HMBC NMR spectrum of compound **1** (mixture of *Z* and *E* isomers) in CD_3CN

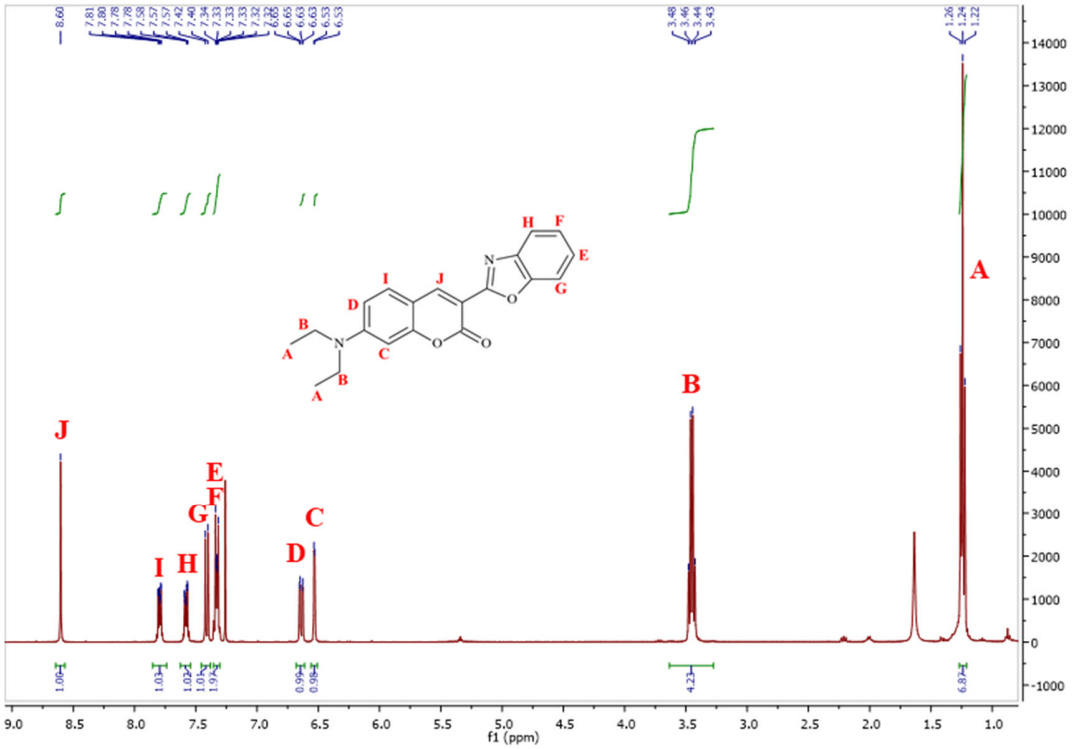

Figure S11. ^{1}H NMR spectrum of compound **2**

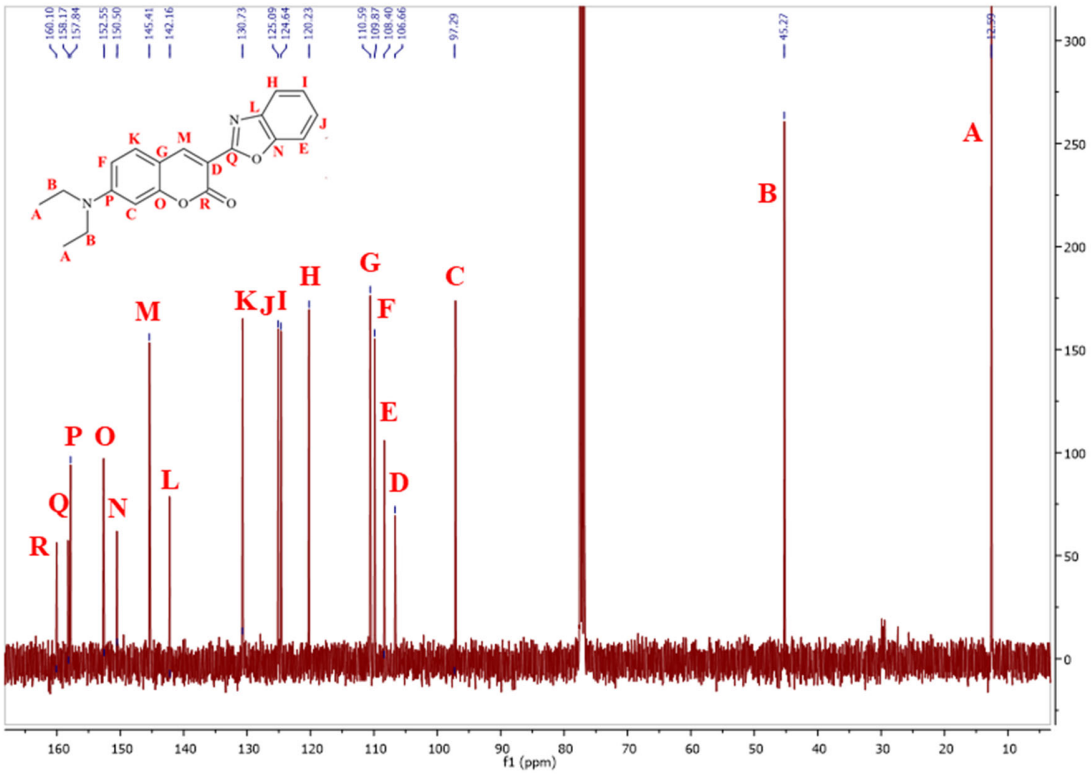

Figure S12. ^{13}C NMR spectrum of compound **2**

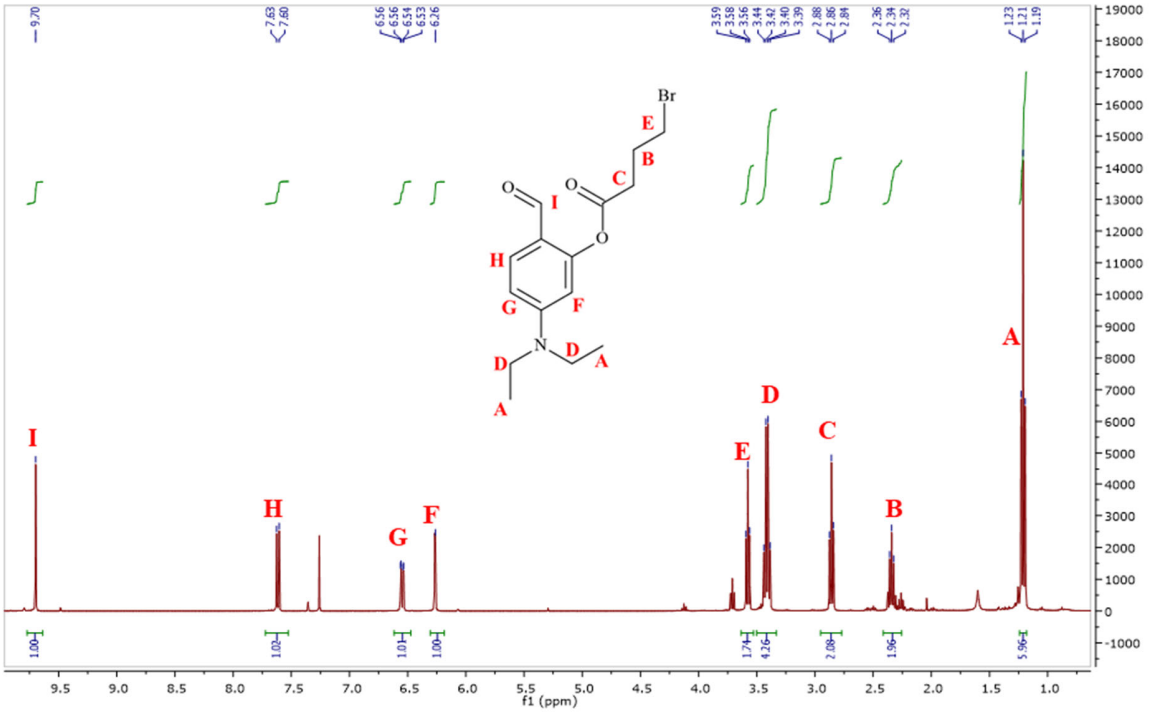

Figure S13. [1]H NMR spectrum of compound **S7**

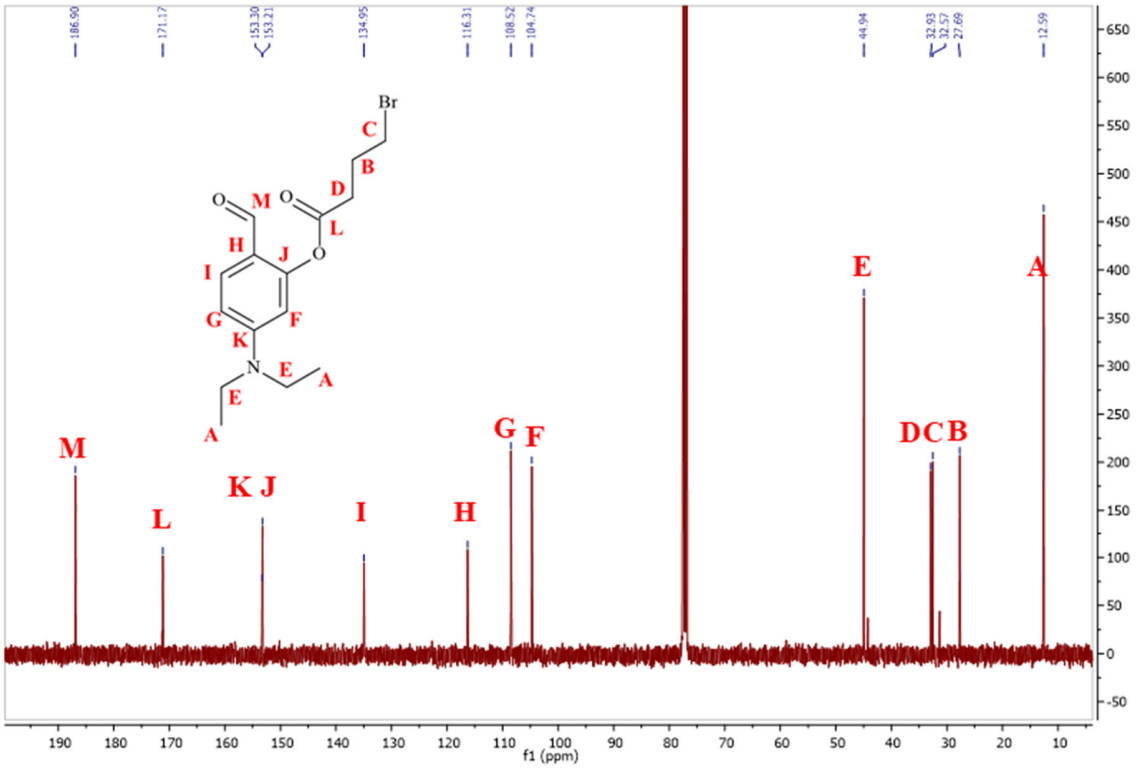

Figure S14. [13]C NMR spectrum of compound **S7**

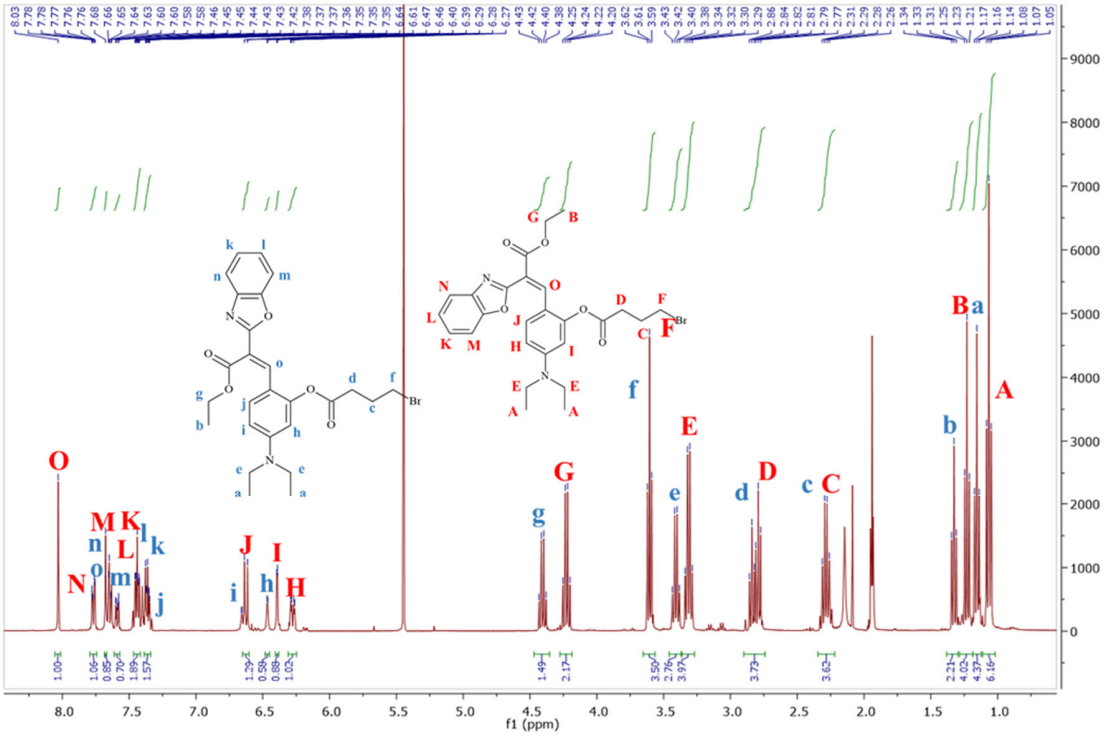

Figure S15. ^{1}H NMR spectrum of compound **1B** (mixture of E:Z isomers) in CD_3CN

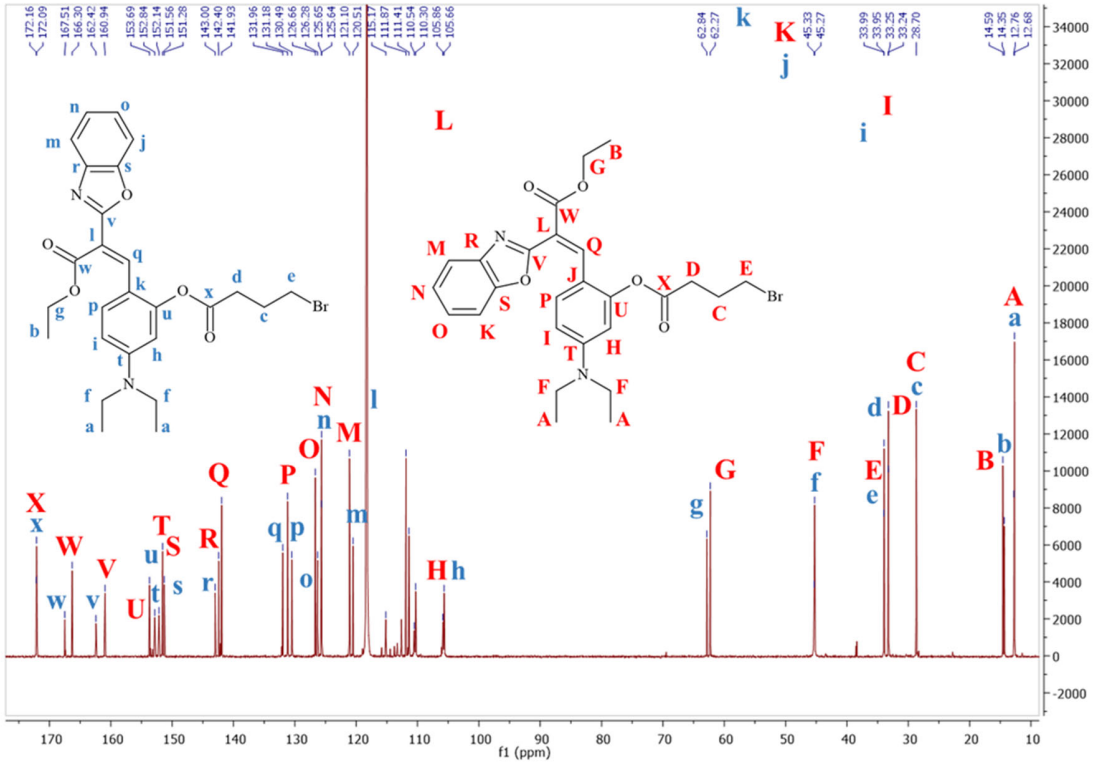

Figure S16. ^{13}C NMR spectrum of compound **1B** (mixture of *Z* and *E* isomers) in CD_3CN

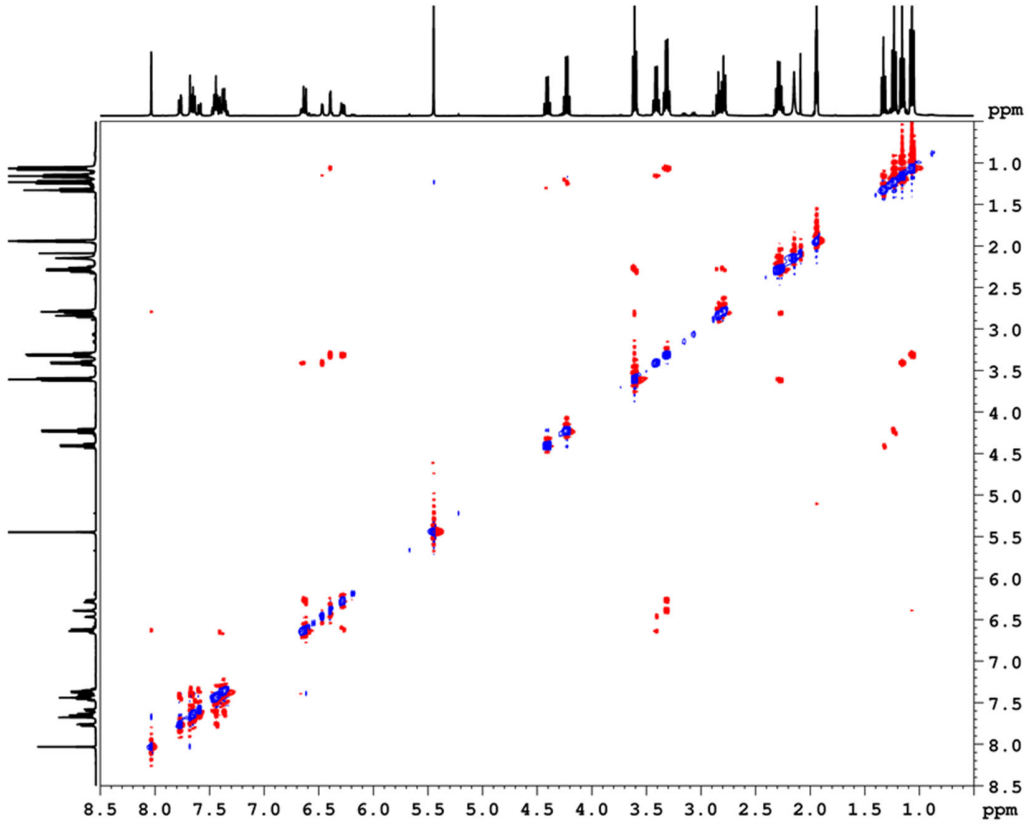

Figure S17. NOESY NMR spectrum of compound **1B** (mixture of *Z* and *E* isomers) in CD_3CN

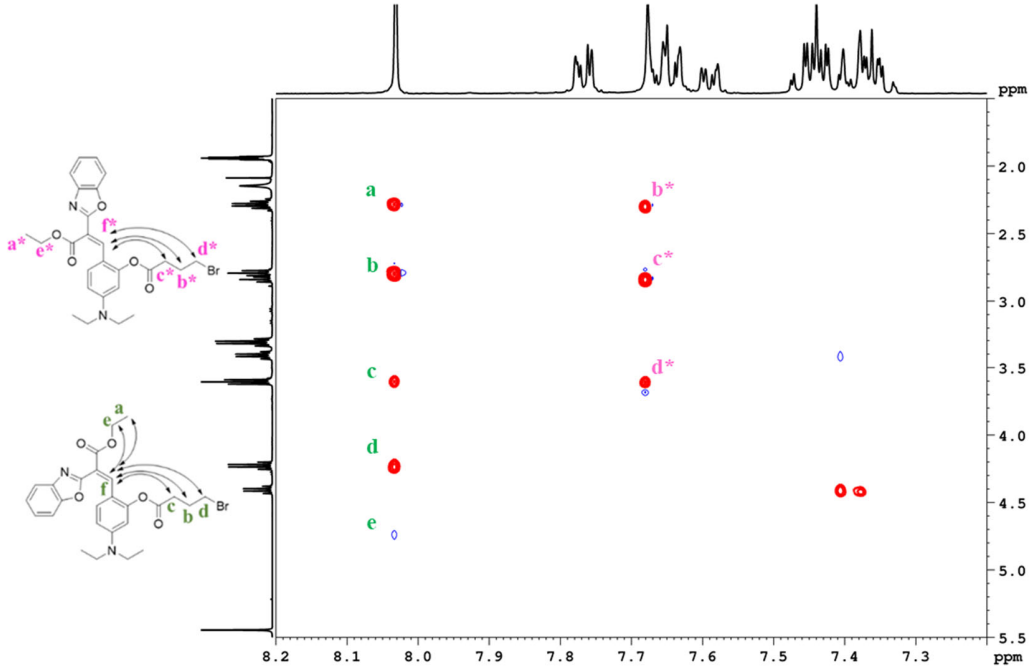

Figure S18. Zoomed-in NOESY NMR spectrum of compound **1B** (mixture of *Z* and *E* isomers) in CD_3CN

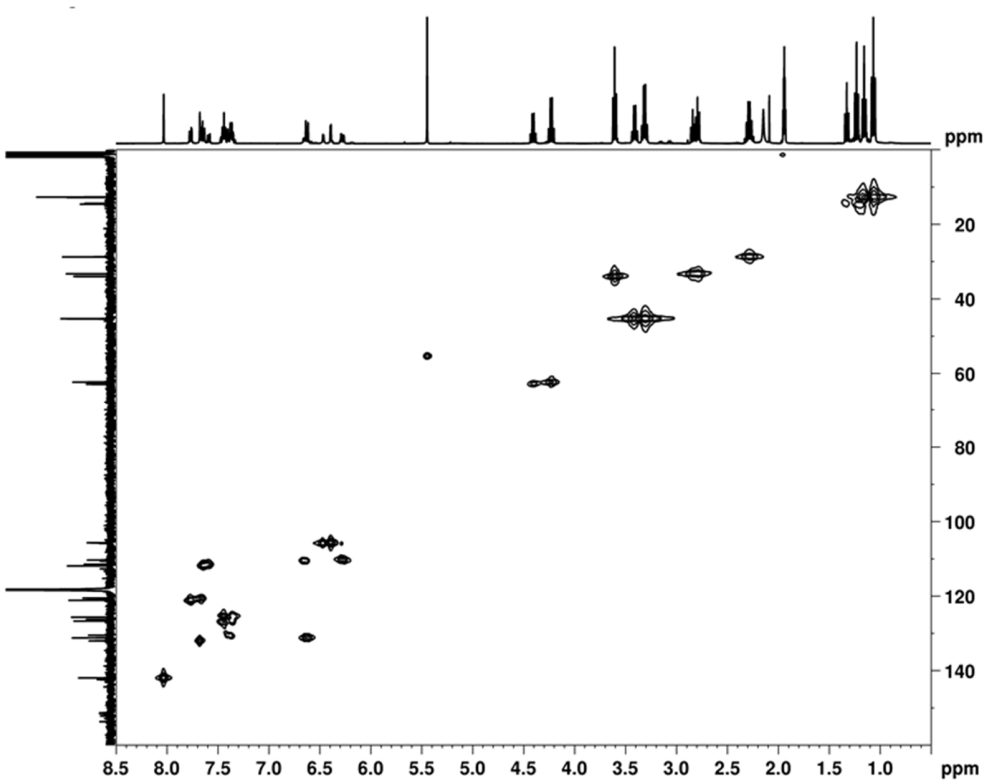

Figure S19. HMQC NMR spectrum of compound **1B** (mixture of *Z* and *E* isomers) in CD_3CN

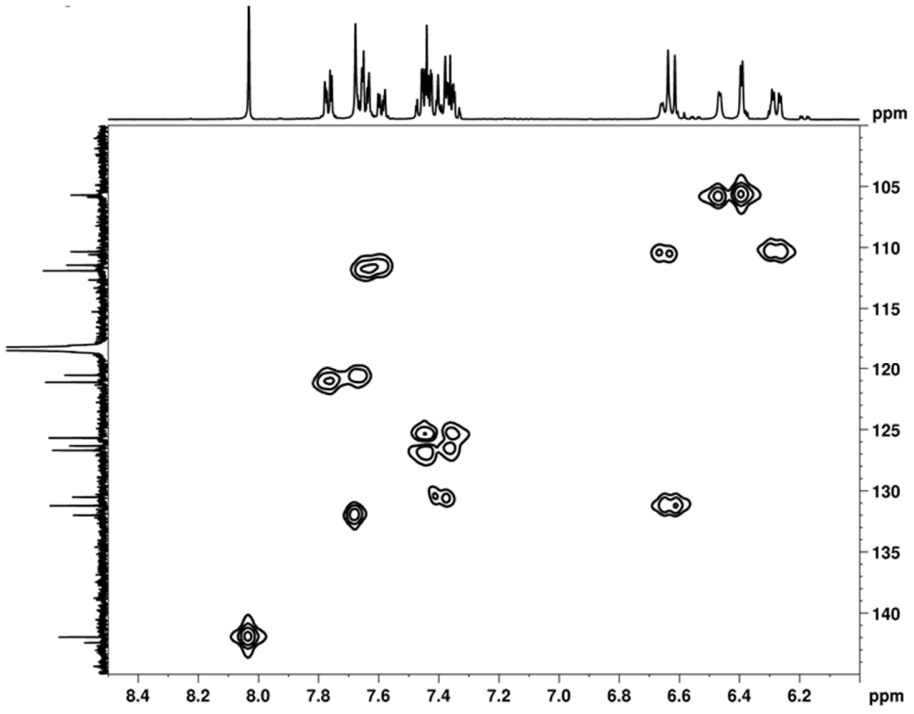

Figure S20. Short-range HMQC NMR spectrum of compound **1B** (mixture of *Z* and *E* isomers) in CD_3CN

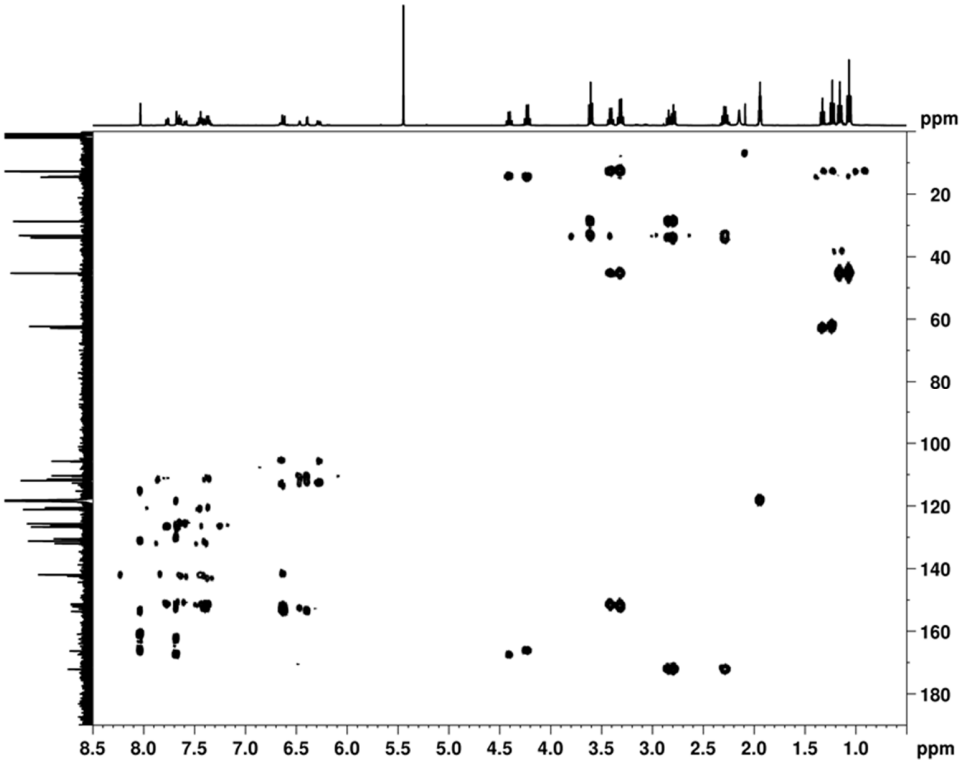

Figure S21. HMBC NMR spectrum of compound **1B** (mixture of *Z* and *E* isomers) in CD_3CN

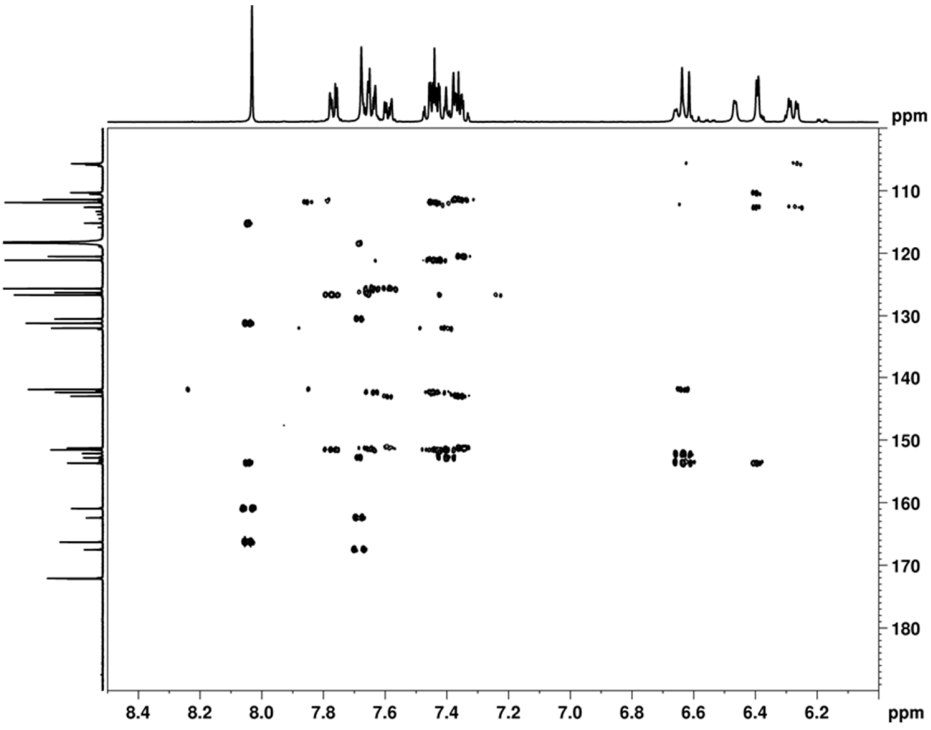

Figure S22. Short-range HMBC NMR spectrum of compound **1B** (mixture of *Z* and *E* isomers) in CD_3CN

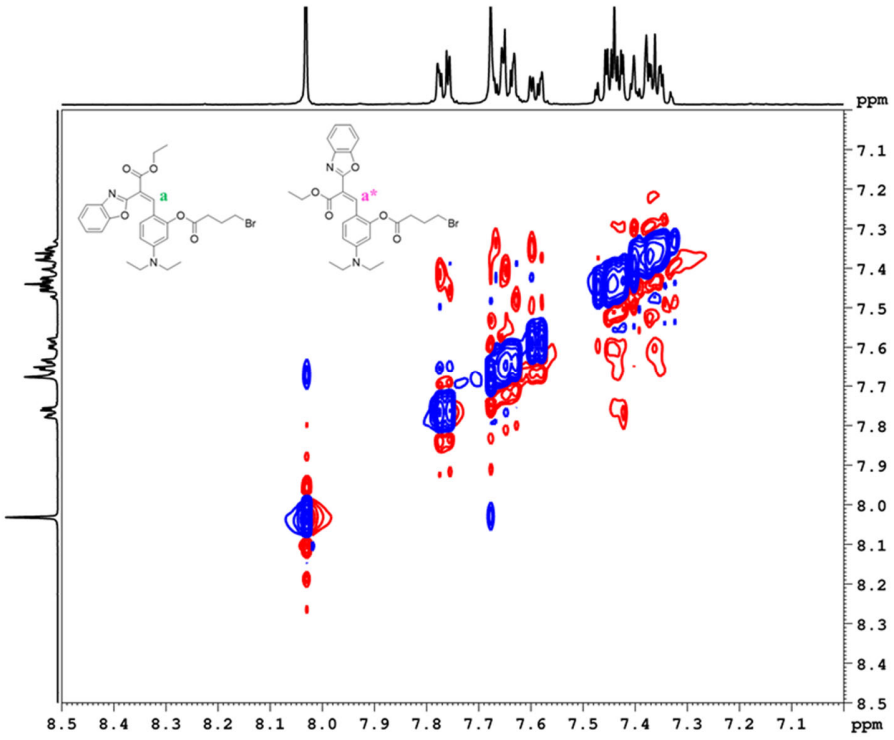

Figure S23. Zoomed-in EXSY spectrum experiment of compound **1B** (mixture of *Z* and *E* isomers) in CD_3CN

[1]H NMR EXPANDED SPECTRA OF OF COMPOUND **1** (MIXTURE OF *E* AND *Z* ISOMERS)

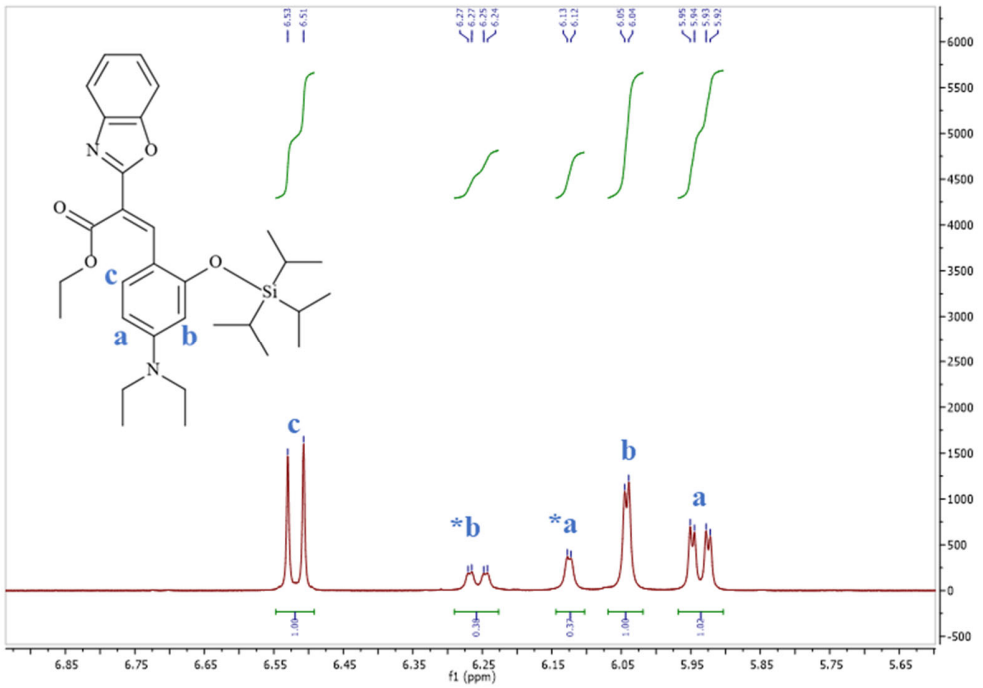

Figure S24. [1]H NMR spectrum of compound **1** (zoomed in on the region between 6.9 and 4.5 ppm; peaks that are starred correspond to the *Z* isomer of compound **1**)

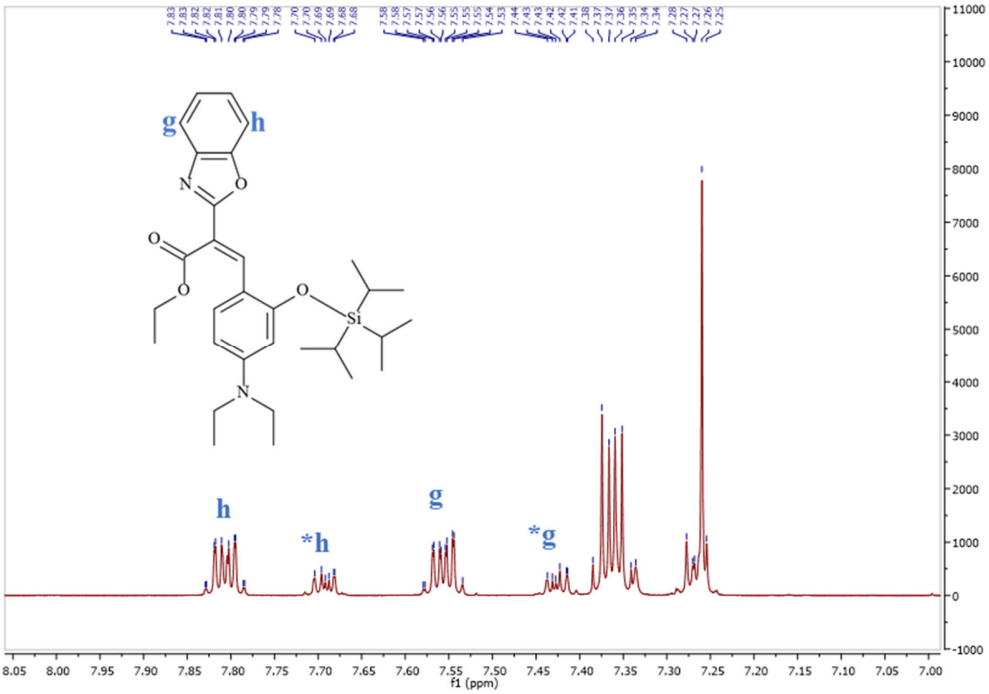

Figure S25. [1]H NMR spectrum of compound **1** (zoomed in on the region between 7.8 and 7.1 ppm; peaks that are starred correspond to the minor Z of compound **1**)

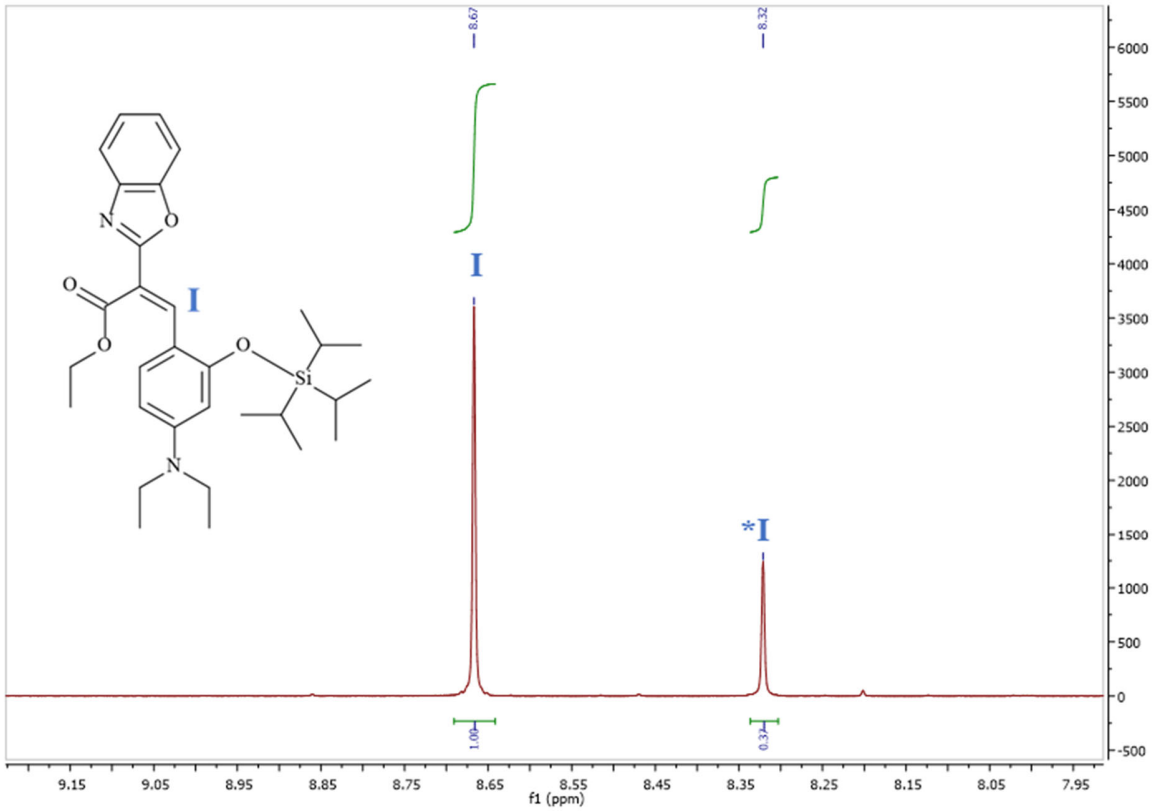

Figure S26. ^{1}H NMR spectrum of compound **1** (*Z* + *E* mixture, zoomed in on the region between 8.9 and 8.0 ppm; peaks that are starred correspond to the Z isomer of compound **1**)

[1]H NMR SPECTRAL TITRATION STUDIES

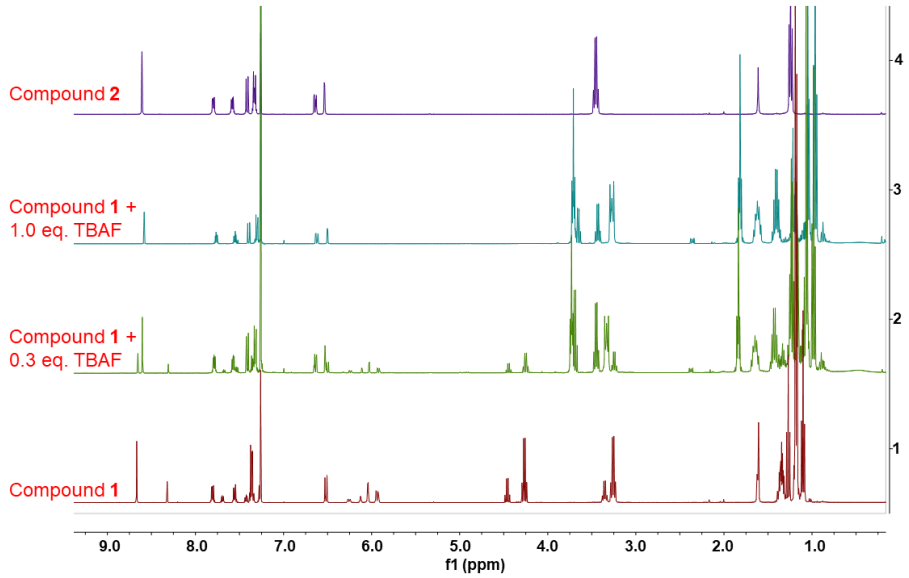

Figure S27. [1]H NMR spectrum titration of compound **1** upon the addition of 0, 0.3, and 1.0 equivalents of TBAF

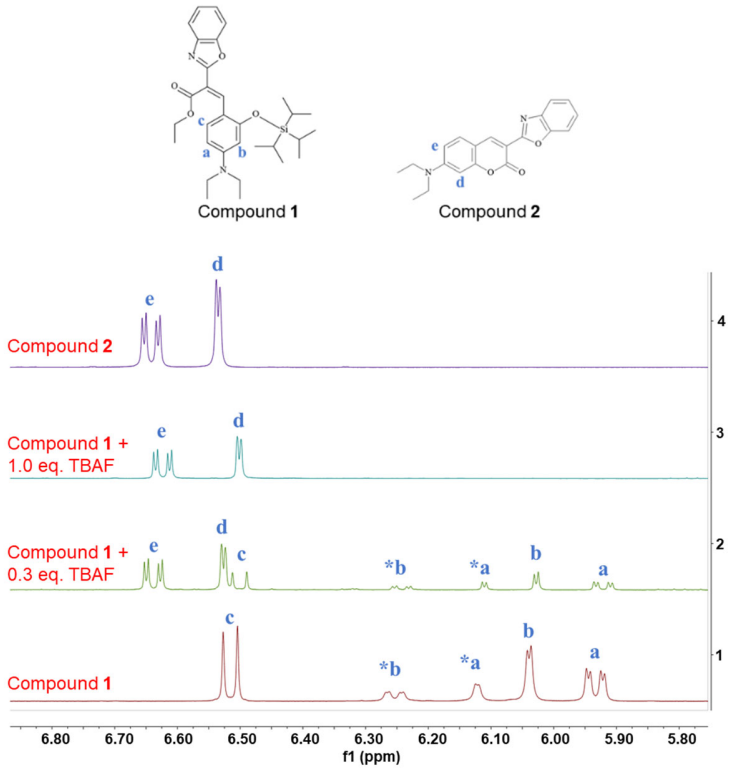

Figure S28. [1]H NMR spectrum titration of compound **1** (*Z* + *E* mixture) upon the addition of 0, 0.3, and 1.0 equivalents of TBAF (zoomed in on the region between 6.9 and 5.7 ppm; starred peaks correspond to the *Z* isomer of compound **1**)

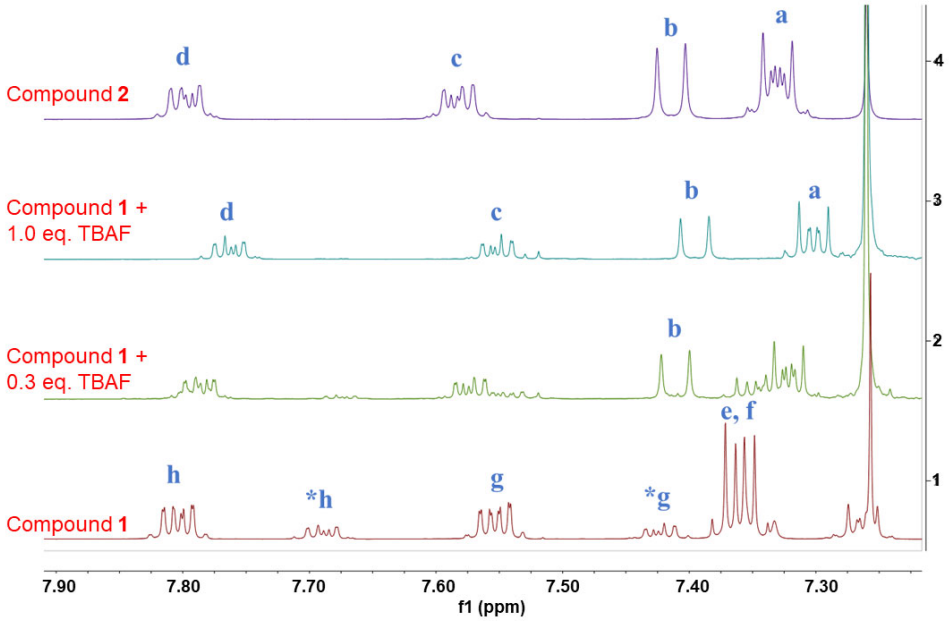

Figure S29. ^{1}H NMR spectrum titration of compound **1** (*Z* + *E* mixture) upon the addition of 0, 0.3, and 1.0 equivalents of TBAF (zoomed in on the region between 8.0 and 7.2 ppm; starred peaks correspond to the *Z* isomer of compound **1**)

SELECTIVITY STUDIES

4 micromolar solutions

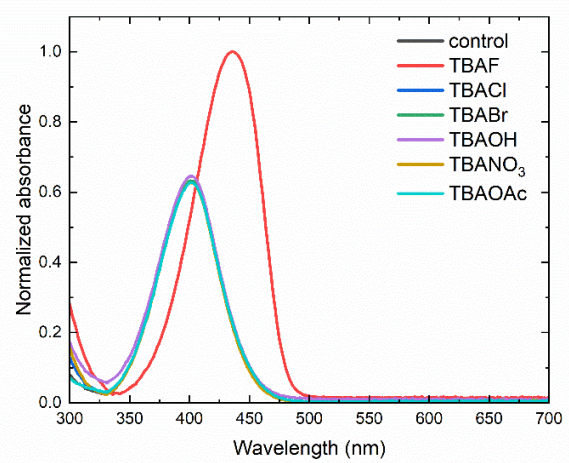

Figure S30. UV-vis absorbance spectra of acetonitrile solutions of compound **1** after exposure to various analytes ([**1**] = 4 μM; [analyte] = 4 μM)

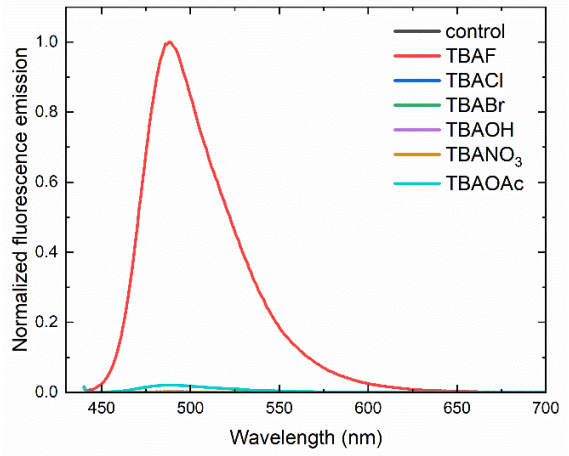

Figure S31. Fluorescence emission spectra of acetonitrile solutions of compound **1** after exposure to various analytes ([**1**] = 4 μM; [analyte] = 4 μM)

10 micromolar solutions

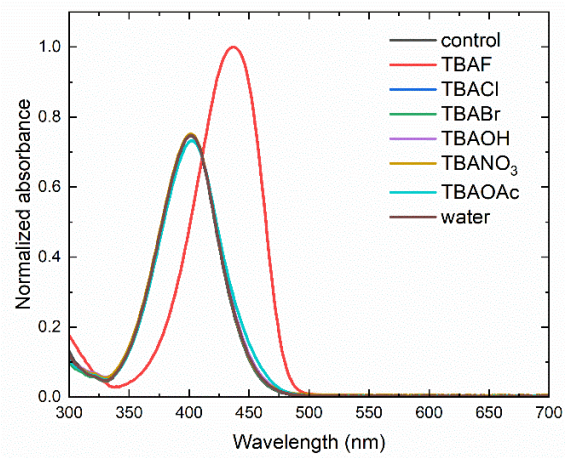

Figure S32. UV-vis absorbance spectra of acetonitrile solutions of compound **1** after exposure to various analytes ([**1**] = 10 μM; [analyte] = 10 μM)

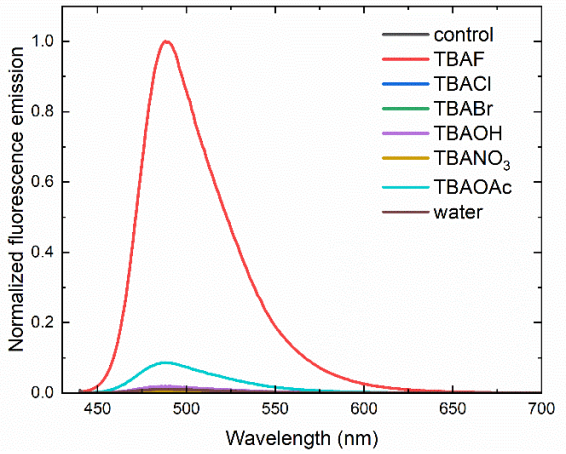

Figure S33. Fluorescence emission spectra of acetonitrile solutions of compound **1** after exposure to various analytes ([**1**] = 10 μM; [analyte] = 10 μM)

COMPETITION STUDIES

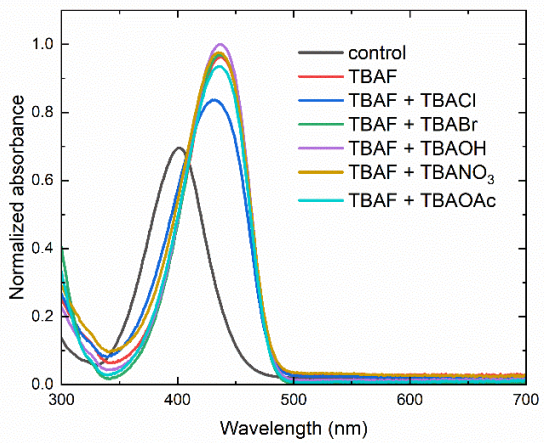

Figure S34. UV-vis absorbance spectra of acetonitrile solutions of compound **1** after exposure to various analytes ([**1**] = 4 μM; [analyte] = 4 μM)

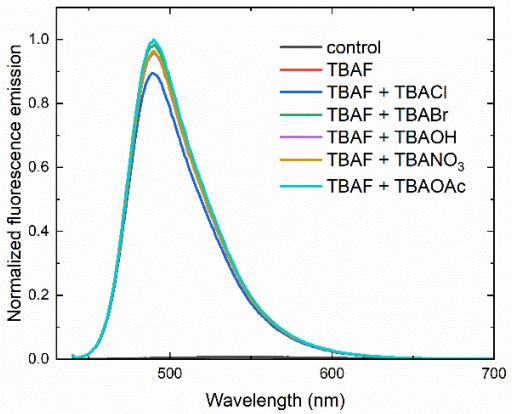

Figure S35. Fluorescence emission spectra of acetonitrile solutions of compound **1** after exposure to various analytes ([**1**] = 4 μM; [analyte] = 4 μM)

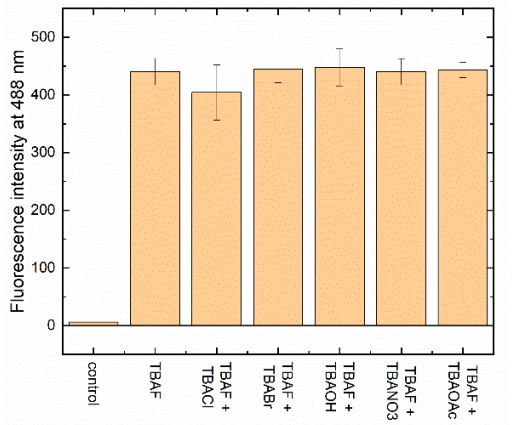

Figure S36. Fluorescence intensity of acetonitrile solutions of compound **1** in the presence of TBAF and other, potentially competing analytes (([**1**] = 4 μM ; [analyte] = 4 μM)

LIMIT OF DETECTION STUDIES

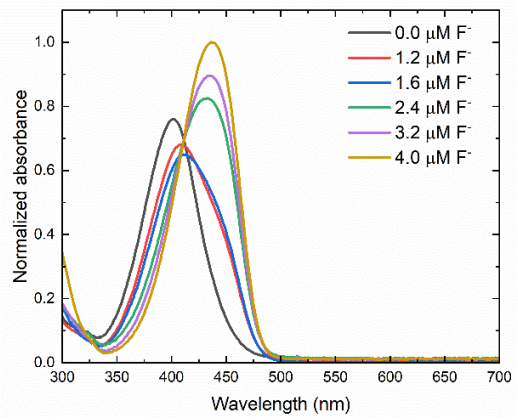

Figure S37. UV-vis absorbance spectra of acetonitrile solutions of compound **1** after exposure to increasing concentrations of fluoride ([**1**] = 4 μM)

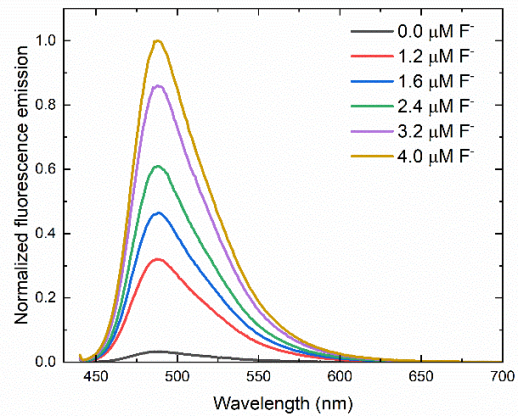

Figure S38. Fluorescence emission spectra of acetonitrile solutions of compound **1** after exposure to increasing concentrations of fluoride ([**1**] = 4 μM)

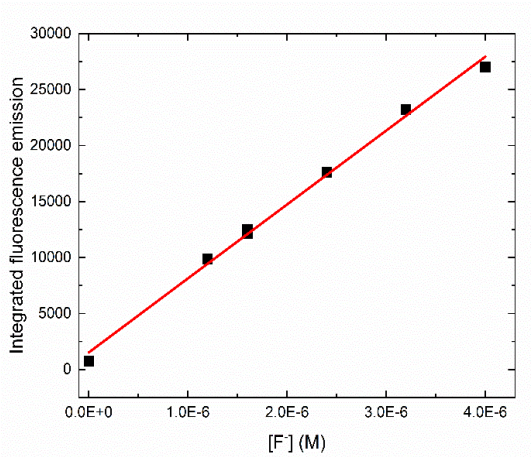

Figure S39. Best linear fit of the integrated fluorescence data of compound **1** as a function of increasing concentrations of F^- ([**1**] = 4 μM; y = 7E+09x + 1524; R^2 = 0.9952)

REAL-WORLD SAMPLE STUDIES

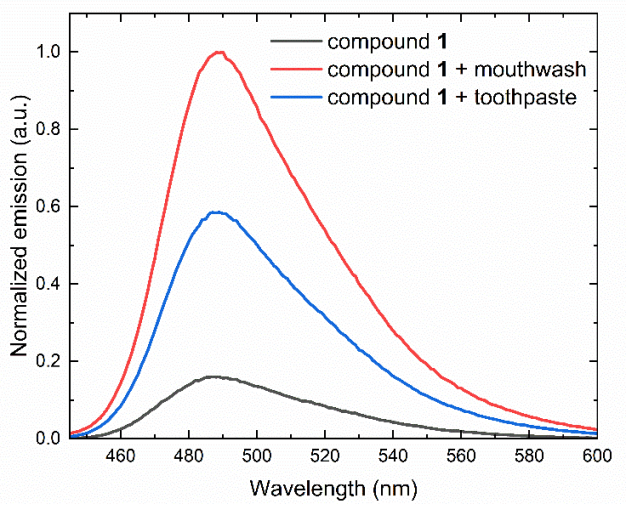

Figure S40. Fluorescence emission spectra of solutions of compound **1** ([**1**] = 4 μM in acetonitrile) in the absence of any sample (grey line), and in the presence of fluoridated mouthwash (red line) and fluoride-containing toothpaste (blue line)

Figure S41. Photographs of the commercial fluoride-containing products, showing that both products have fluoride listed as a key component

Figure S42. Photograph of solutions of compound **1** without analyte, and in the presence of mouthwash and toothpaste, taken under 365 nm excitation ([**1**] = 4 μM in acetonitrile)

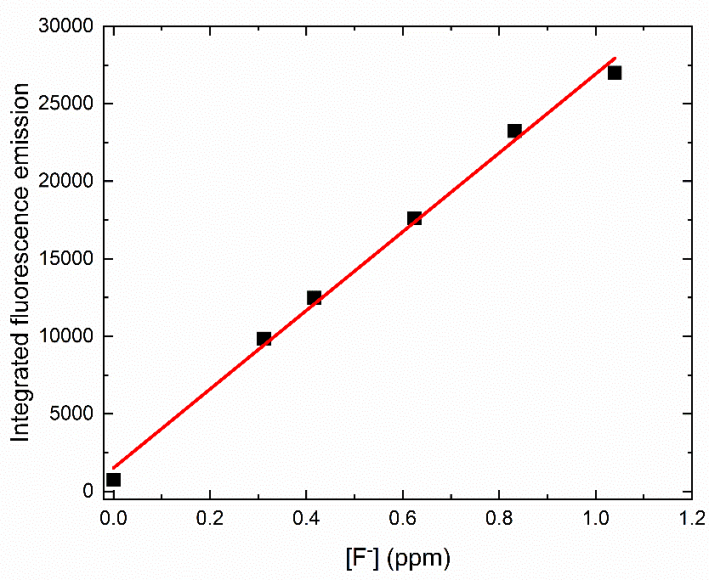

Figure S43. Calibration curve plotting the concentration of fluoride ion (in ppm) on the X-axis vs. the integrated fluorescence emission of solutions of compound **1** on the Y-axis, used for the quantification of the fluoride concentration in real-world samples

KINETIC STUDIES

*At room temperature and 10 µM of compound **1** after the addition of 4 µM of TBAF*

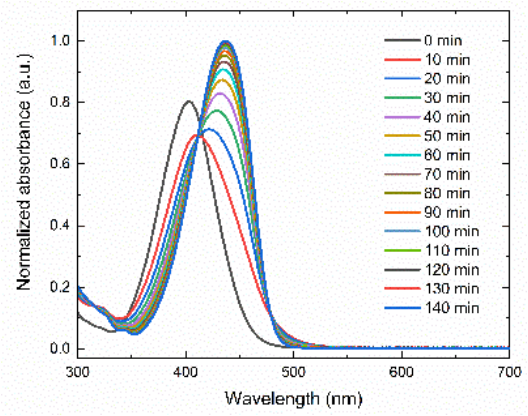

Figure S44. UV-vis absorbance of acetonitrile solutions of compound **1** as a function of time ([**1**] = 10 µM; room temperature)

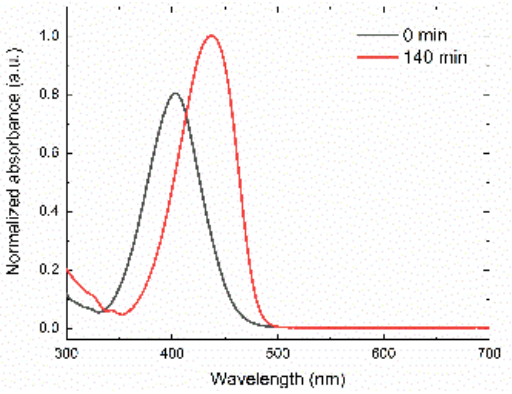

Figure S45. Summary figure of the UV-vis absorbance of acetonitrile solutions of compound **1** as a function of time ([**1**] = 10 µM; room temperature)

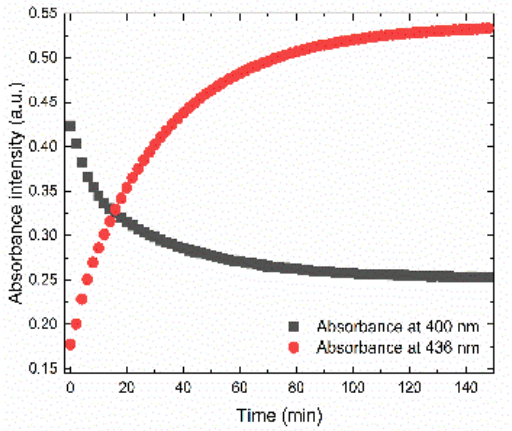

Figure S46. UV-vis absorbance of acetonitrile solutions of compound **1** at 436 nm and at 400 nm as a function of time ([**1**] = 10 µM; room temperature)

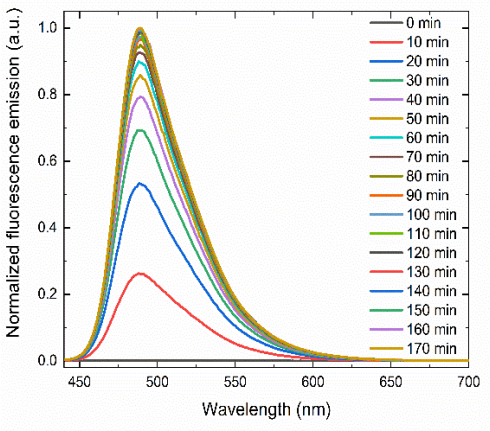

Figure S47. Fluorescence emission spectra of acetonitrile solutions of compound **1** as a function of time ([**1**] = 10 μM; room temperature)

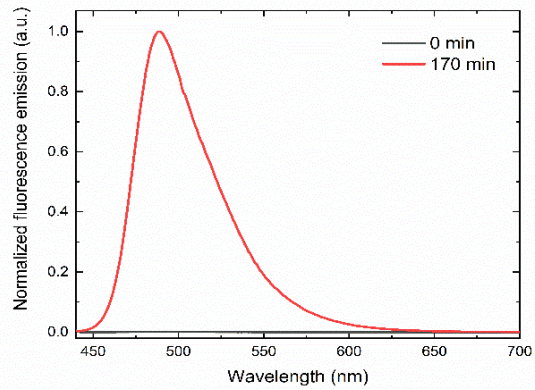

Figure S48. Summary figure of the fluorescence emission spectra of acetonitrile solutions of compound **1** as a function of time ([**1**] = 10 μM; room temperature)

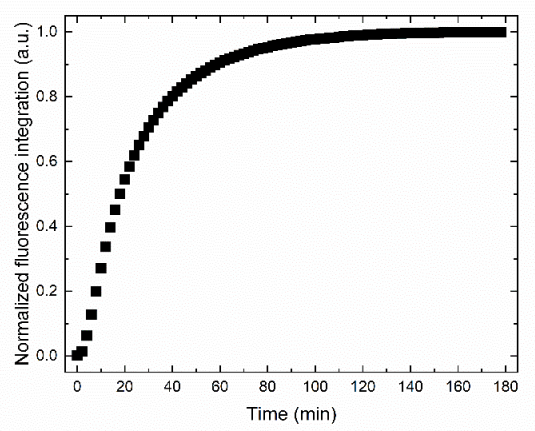

Figure S49. Integrated fluorescence emission spectra of acetonitrile solutions of compound **1** as a function of time ([**1**] = 10 μM; room temperature)

*At room temperature and 4 μM of compound **1** after the addition of 4 μM of TBAF*

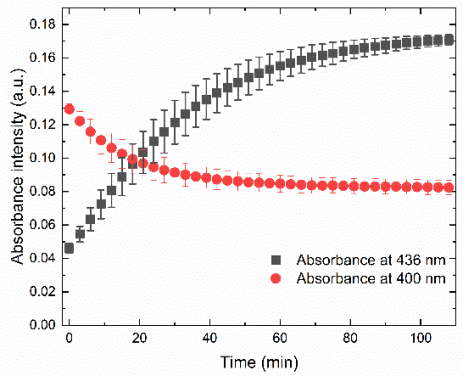

Figure S50. UV-vis absorbance of acetonitrile solutions of compound **1** at 436 nm and at 400 nm as a function of time ([**1**] = 4 μM; room temperature; results represent an average of 3 trials).

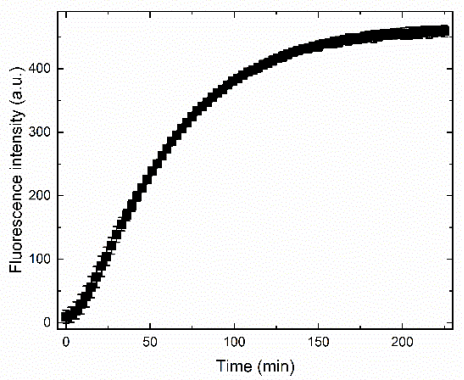

Figure S51. Fluorescence intensity of acetonitrile solutions of compound **1** at 488 nm as a function of time ([**1**] = 4 μM; room temperature; results represent an average of 3 trials).

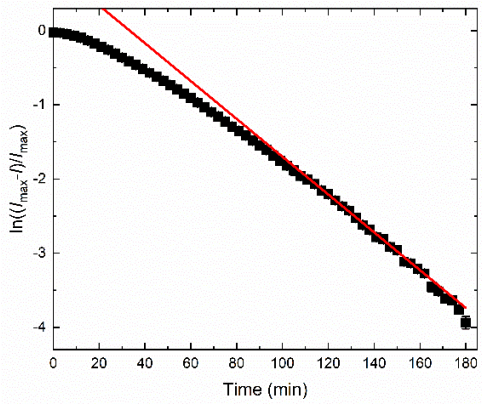

Figure S52. Best fit of fluorescence intensity of acetonitrile solutions of compound **1** to a first-order reaction equation ([**1**] = 4 μM; room temperature; fluorescence intensity measured at 488 nm; Y-axis: $\ln(I_{max}-I)/I_{max}$); linear fit equation: y = -0.0218x + 0.307; R^2 = 0.9896; results represent an average of 3 trials)

*At room temperature and 4 μM of compound **1** after the addition of 8 μM of TBAF*

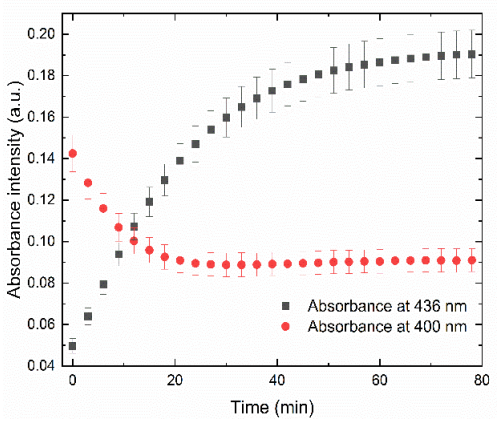

Figure S53. UV-vis absorbance of acetonitrile solutions of compound **1** at 436 nm and at 400 nm as a function of time ([**1**] = 4 μM; room temperature; results represent an average of 3 trials).

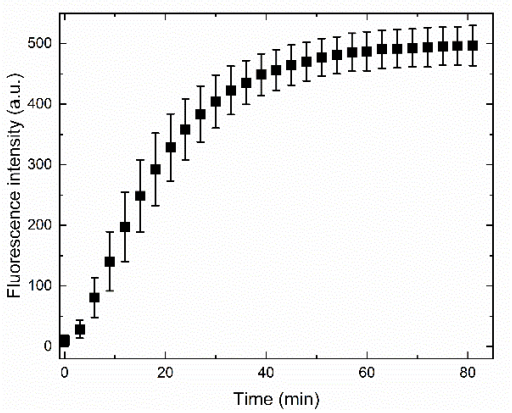

Figure S54. Fluorescence intensity of acetonitrile solutions of compound **1** at 488 nm as a function of time ([**1**] = 4 μM; room temperature; results represent an average of 3 trials)

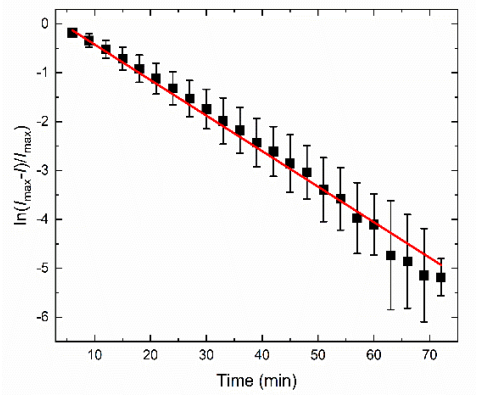

Figure S55. Best fit of fluorescence intensity of acetonitrile solutions of compound **1** to a first-order reaction equation ([**1**] = 4 μM; room temperature; fluorescence intensity measured at 488 nm; Y-axis: $\ln(I_{max}-I)/I_{max}$); linear fit equation: y = -0.0759x + 0.3917; R^2 = 0.9886; results represent an average of 3 trials)

*At room temperature and 2 μM of compound **1** after the addition of 4 μM of TBAF*

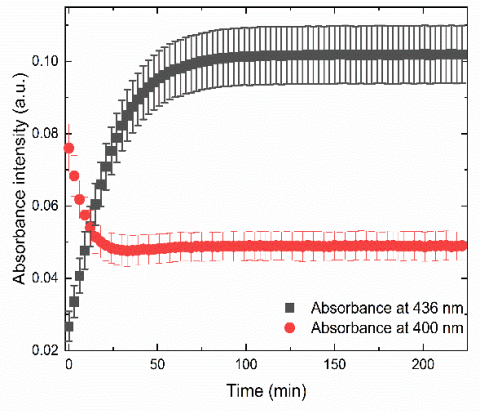

Figure S56. UV-vis absorbance of acetonitrile solutions of compound **1** at 436 nm and at 400 nm as a function of time ([**1**] = 4 μM; room temperature; results represent an average of 3 trials).

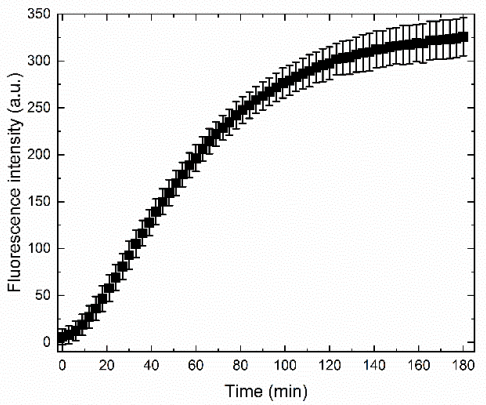

Figure S57. Fluorescence intensity of acetonitrile solutions of compound **1** at 488 nm as a function of time ([**1**] = 4 μM; room temperature; results represent an average of 3 trials).

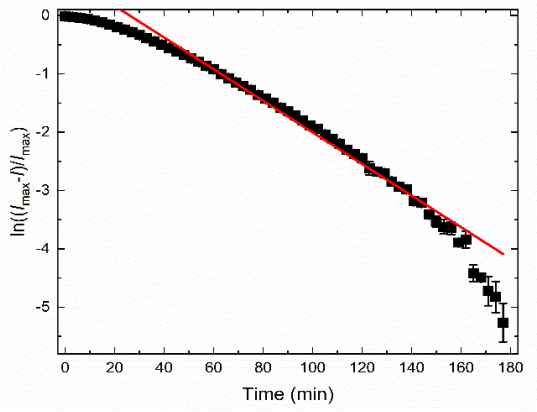

Figure S58. Best fit of fluorescence intensity of acetonitrile solutions of compound **1** to a first-order reaction equation ([**1**] = 4 μM; room temperature; fluorescence intensity measured at 488 nm; Y-axis: $\ln(I_{max}-I)/I_{max}$); linear fit equation: y = -0.0269x + 0.5361; R^2 = 0.9598; results represent an average of 3 trials)

*At 40 °C and 4 μM of compound **1** after the addition of 4 μM of TBAF*

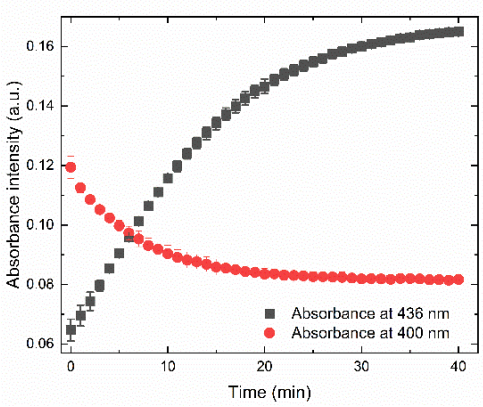

Figure S59. UV-vis absorbance of acetonitrile solutions of compound **1** at 436 nm and at 400 nm as a function of time ([**1**] = 4 μM; 40 °C; results represent an average of 3 independent trials)

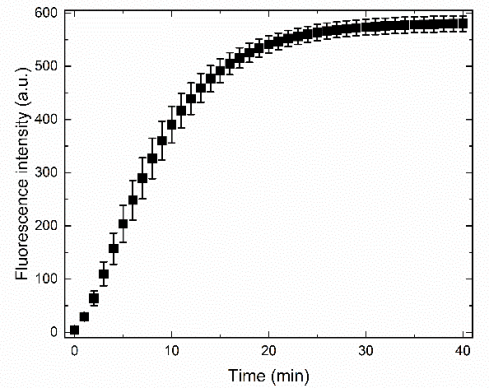

Figure S60. Fluorescence intensity of acetonitrile solutions of compound **1** at 488 nm as a function of time ([**1**] = 4 μM; 40 °C; results represent an average of 3 independent trials)

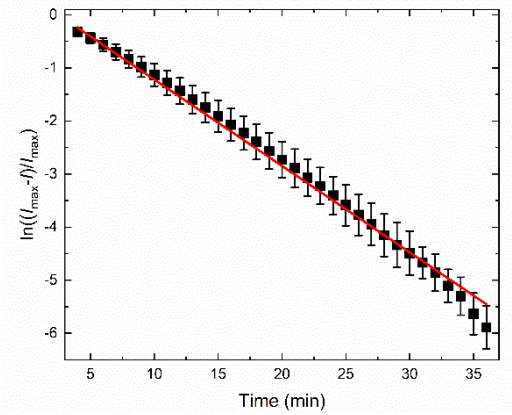

Figure S61. Best fit of fluorescence intensity of acetonitrile solutions of compound **1** to a first-order reaction equation ([**1**] = 4 μM; 40 °C; fluorescence intensity measured at 488 nm; Y-axis: $\ln(I_{max}-I)/I_{max}$); linear fit equation: y = -0.1702x + 0.5783; R^2 = 0.9953; results represent an average of 3 independent trials)

COLORIMETRIC STUDIES

Solution-state colorimetric studies

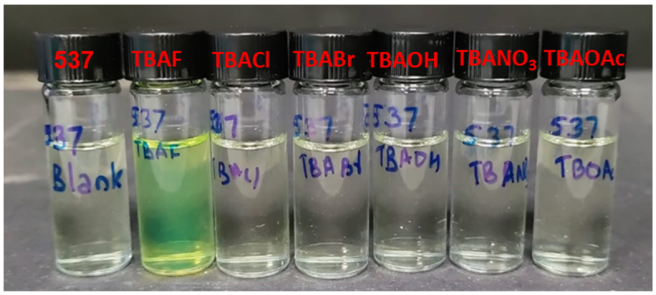

Figure S62. Images taken under ambient light of solutions of compound **1**, followed by exposure to no analyte (left-most vial), or exposure to analytes: TBAF, TBACl, TBABr, TBAOH, $TBANO_3$, or TBAOAc ([**1**] = 10 μM; [analyte] = 10 μM)

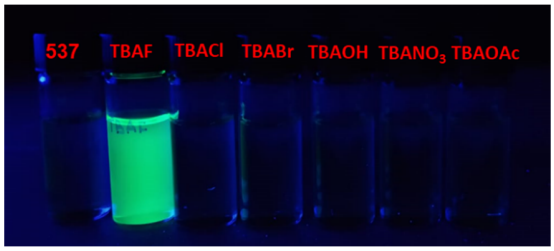

Figure S63. Images taken under excitation with a hand-held long-wave TLC lamp (excitation at 365 nm) of solutions of compound **1**, followed by exposure to no analyte (left-most vial), or exposure to analytes: TBAF, TBACl, TBABr, TBAOH, $TBANO_3$, or TBAOAc ([**1**] = 10 μM; [analyte] = 10 μM)

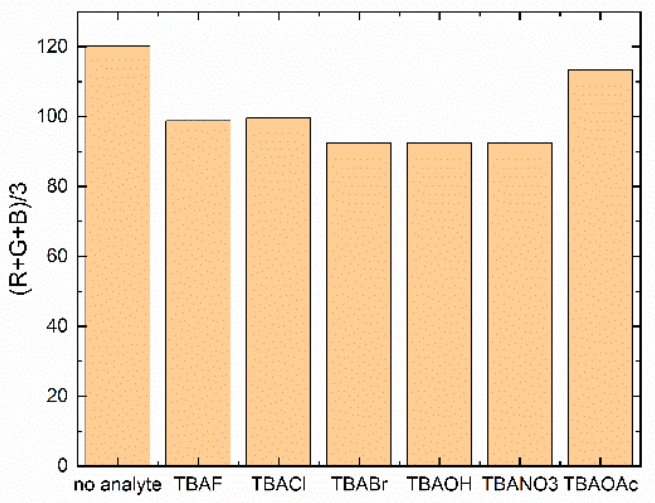

Figure S64. Summary of the quantitative colorimetric data ((R+G+B)/3) of images of solutions of compound **1**, photographed under ambient light, after exposure to no analyte, or exposure to analytes: TBAF, TBACl, TBABr, TBAOH, $TBANO_3$, or TBAOAc ([**1**] = 10 μM; [analyte] = 10 μM)

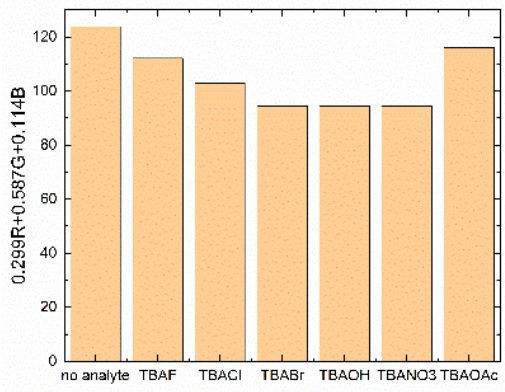

Figure S65. Summary of the quantitative colorimetric data (0.299R+0.587G+0.114B) of images of solutions of compound **1**, photographed under ambient light, after exposure to no analyte, or exposure to analytes: TBAF, TBACl, TBABr, TBAOH, $TBANO_3$, or TBAOAc ([**1**] = 10 μM; [analyte] = 10 μM)

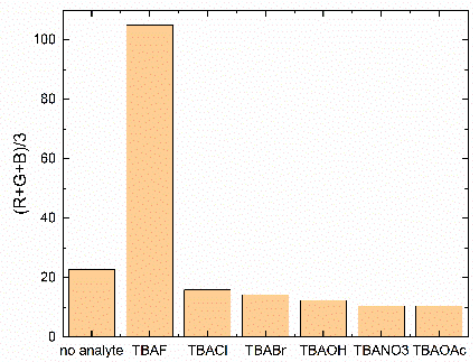

Figure S66. Summary of the quantitative colorimetric data ((R+G+B)/3) of images of solutions of compound **1**, photographed under excitation with 365 nm light, after exposure to no analyte, or exposure to analytes: TBAF, TBACl, TBABr, TBAOH, $TBANO_3$, or TBAOAc ([**1**] = 10 μM; [analyte] = 10 μM)

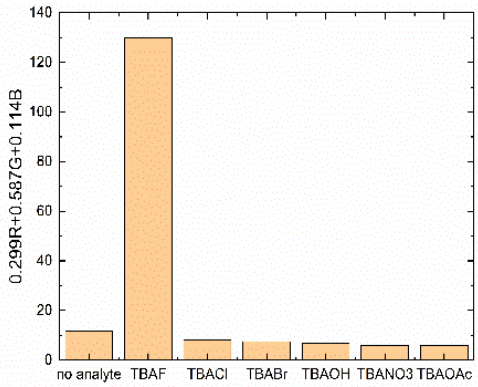

Figure S67. Summary of the quantitative colorimetric data (0.299R+0.587G+0.114B) of images of solutions of compound **1**, photographed under excitation with 365 nm light, after exposure to no analyte, or exposure to analytes: TBAF, TBACl, TBABr, TBAOH, $TBANO_3$, or TBAOAc ([**1**] = 10 μM; [analyte] = 10 μM)

Solid-state colorimetric studies

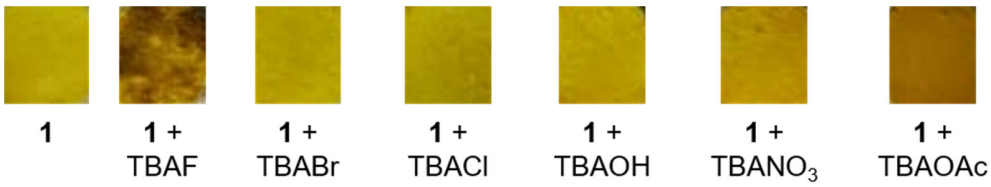

Figure S68. Images taken under ambient light of filter paper onto which compound **1** was adsorbed, followed by exposure to no analyte (left-most panel), or exposure to analytes: TBAF, TBABr, TBACl, TBAOH, $TBANO_3$, or TBAOAc ([**1**] = 6 mM; [analyte] = 6 mM)

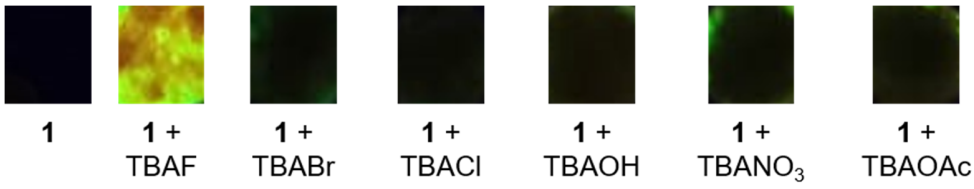

Figure S69. Images taken under excitation with a hand-held long-wave TLC lamp (excitation at 365 nm) of filter paper onto which compound **1** was adsorbed, followed by exposure to no analyte (left-most panel), or exposure to analytes: TBAF, TBABr, TBACl, TBAOH, $TBANO_3$, or TBAOAc ([**1**] = 6 mM; [analyte] = 6 mM)

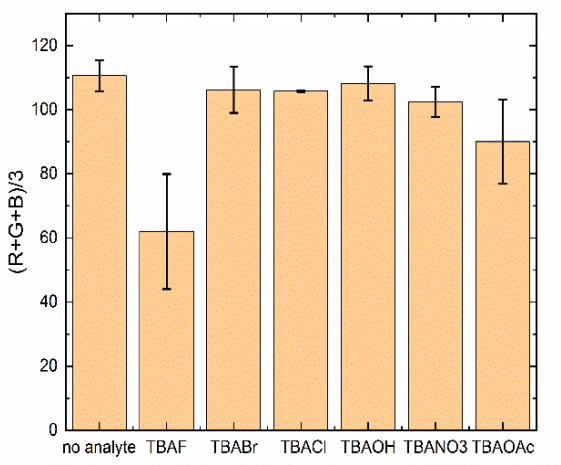

Figure S70. Summary of the quantitative colorimetric data ((R+G+B)/3) of images of filter paper onto which compound **1** was adsorbed, photographed under ambient light, after exposure to no analyte, or exposure to analytes: TBAF, TBABr, TBACl, TBAOH, $TBANO_3$, or TBAOAc ([**1**] = 6 mM; [analyte] = 6 mM)

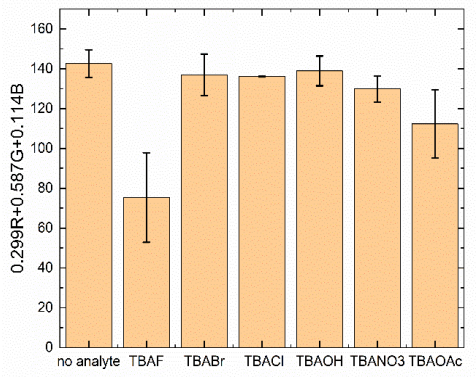

Figure S71. Summary of the quantitative colorimetric data (0.299R+0.587G+0.114B) of images of filter paper onto which compound **1** was adsorbed, photographed under ambient light, after exposure to no analyte, or exposure to analytes: TBAF, TBABr, TBACl, TBAOH, $TBANO_3$, or TBAOAc ([**1**] = 6 mM; [analyte] = 6 mM)

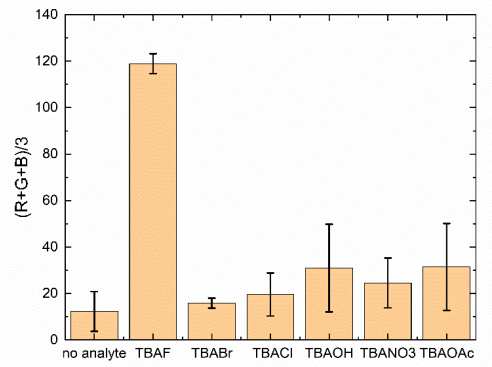

Figure S72. Summary of the quantitative colorimetric data ((R+G+B)/3) of images of filter paper onto which compound **1** was adsorbed, photographed under excitation with 365 nm light, after exposure to no analyte, or exposure to analytes: TBAF, TBABr, TBACl, TBAOH, $TBANO_3$, or TBAOAc ([**1**] = 6 mM; [analyte] = 6 mM)

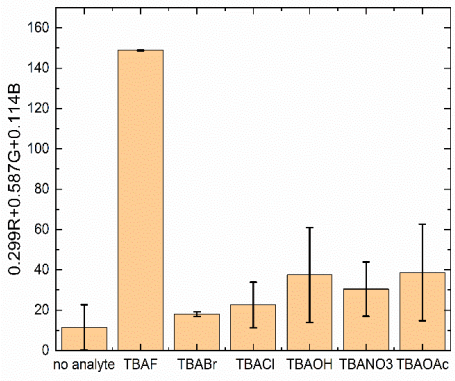

Figure S73. Summary of the quantitative colorimetric data (0.299R+0.587G+0.114B) of images of filter paper onto which compound **1** was adsorbed, photographed under excitation with 365 nm light, after exposure to no analyte, or exposure to analytes: TBAF, TBABr, TBACl, TBAOH, $TBANO_3$, or TBAOAc ([**1**] = 6 mM; [analyte] = 6 mM)

HPLC STUDIES

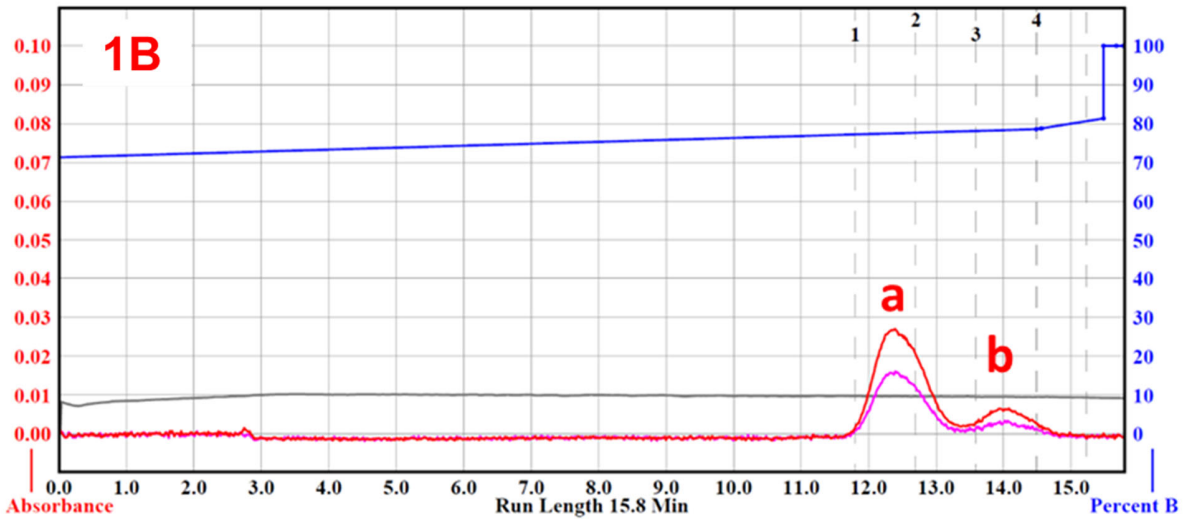

Figure S74. HPLC chromatogram of compound **1B**, showing the presence of two isomers (shown as "a" and "b" in the chromatogram above; confirmed as the *E* isomer (peak "a") and *Z* isomer (peak "b").

REFERENCES

[1] Lakowicz, J. R. *Principles of Fluorescence Spectroscopy*, Springer: New York USA, **2006**; DOI: 10.1007/978-0-387-46312-4.

[2] Brouwer, A. M. Standards for Photoluminescence Quantum Yield Measurements in Solution (IUPAC Technical Report). *Pure Appl. Chem.* **2011**, *83*, 2213-2228; DOI: 10.1351/PAC-REP-10-09-31.

[3] Saute, B.; Premasiri, R.; Ziegler, L.; Narayanan, R. Gold Nanorods as Surface Enhanced Raman Spectroscopy Substrates for Sensitive and Selective Detection of Ultra-Low Levels of Dithiocarbamate Pesticides. *Analyst* **2012**, *137*, 5082-5087; DOI: 10.1039/C2AN36047K.

[4] da Hora Machado, A. E.; Severino, D.; Ribeiro, J.; De Paula, R.; Gehlen, M. H.; de Oliveira, H. P. M.; dos Santos Matos, M.; de Miranda, J. A. Solvent Effects on the Photophysics of 3-(Benzoxazol-2-yl)-7-(*N,N*-diethylamino)chromen-2-one. *Photochem. Photobiol. Sci.* **2004**, *3*, 79-84; DOI: 10.1039/B308121D.

[5] Zhu, B.; Yuan, F.; Li, R.; Li, Y.; Wei, Q.; Ma, Z.; Du, B.; Zhang, X. A Highly Selective Colorimetric and Ratiometric Fluorescent Chemodosimeter for Imaging Fluoride Ions in Living Cells. *Chem. Commun.* **2011**, *47*, 7098-7100; DOI: 10.1039/c1cc11308a.

[6] Wei, G.; Yin, J.; Ma, X.; Yu, S.; Wei, D.; Du, Y. A Carbohydrate Modified Fluoride Ion Sensor and its Applications. *Anal. Chim. Acta* **2011**, *703*, 219-225; DOI: 10.1016/j.aca.2011.07.009.

[7] Sokkalingam, P.; Lee, C.-H. Highly Sensitive Fluorescence "Turn-on" Indicator for Fluoride Anion with Remarkable Selectivity in Organic and Aqueous Media. *J. Org. Chem.* **2011**, *76*, 3820-3828; DOI: 10.1021/jo200138t.

[8] Cao, X.; Lin, W.; Yu, Q.; Wang, J. Ratiometric Sensing of Fluoride Anions Based on a BODIPY-Coumarin Platform. *Org. Lett.* **2011**, *13*, 6098-6101; DOI: 10.1021/ol202595t.

[9] Bao, Y.; Liu, B.; Wang, H.; Tian, J.; Bai, R. A "Naked Eye" and Ratiometric Fluorescent Chemosensor for Rapid Detection of F^- Based on Combination of Desilylation Reaction and Excited-State Proton Transfer. *Chem. Commun.* **2011**, *47*, 3957-3959; DOI: 10.1039/c1cc00034a.

[10] Fu, L.; Jiang, F.-L.; Fortin, D.; Harvey, P. D.; Liu, Y. A Reaction-Based Chromogenic and Fluorescent Chemodosimeter for Fluoride Anions. *Chem. Commun.* **2011**, *47*, 5503-5505; DOI: 10.1039/c1cc10784d.

[11] Lu, W.; Jiang, H.; Hu, F.; Jiang, L.; Shen, Z. A Novel Chemosensor Based on Fe(III)-Complexation for Selective Recognition and Rapid Detection of Fluoride Anions in Aqueous Media. *Tetrahedron* **2011**, *67*, 7909-7912; DOI: 10.1016/j.tet.2011.08.035.

[12] Rochat, S.; Severin, K. A Simple Fluorescence Assay for the Detection of Fluoride in Water at Neutral pH. *Chem. Commun.* **2011**, *47*, 4391-4393; DOI: 10.1039/c1cc10498e.

[13] Sathish, R. S.; Sujith, U.; Rao, G. N.; Janardhana, C. Fluoride Ion Detection by 8-Hydroxyquinoline-Zr(IV)-EDTA Complex. *Spectrochim. Acta Part A: Molec. Biomolec. Spectroscopy* **2006**, *65*, 565-570; DOI: 10.1016/j.saa.2005.12.011.

[14] Kumar, M.; Kumar, R.; Bhalla, V. F^--Induced "Turn-On" Fluorescent Chemosensor Based on 1,3-*alt*-Thiacalix[4]arene. *Tetrahedron* **2009**, *65*, 4340-4344; DOI: 10.1016/j.tet.2009.03.074.

[15] Chen, Z. J.; Wang, L. M.; Zou, G.; Zhang, L.; Zhang, G. J.; Cai, X. F.; Teng, M. S. Colorimetric and Ratiometric Fluorescent Chemosensor for Fluoride Ion Based on Perylene Diimide Derivatives. *Dyes and Pigments* **2012**, *94*, 410-415; DOI: 10.1016/j.dyepig.2012.01.024.

[16] Mashraqui, S. H.; Ghorpade, S. S.; Tripathi, S.; Britto, S. A New Indole Incorporated Chemosensor Exhibiting Selective Colorimetric and Fluorescence Ratiometric Signaling of Fluoride. *Tetrahedron Lett.* **2012**, *53*, 765-768; DOI: 10.1016/j.tetlet.2011.11.139.

[17] Tavallali, H.; Deilamy-Rad, G.; Parhami, A.; Khalafi-Nezhad, A. A Selective Fluorescent and Colorimetry Competition Assay for Fluoride Ions in DMSO Media Based on 4-Chloro-2,6-*bis*(Hydroxymethyl) Phenol. *J. Anal. Chem.* **2014**, *69*, 157-161; DOI: 10.1134/S1061934814020130.

[18] Li, G.; Gong, W.-T.; Ye, J.-W.; Lin, Y.; Ning, G.-L. Unprecedented Intramolecular Cyclization of Pyridinium to Pyrido[1,2-*a*]Benzimidazole: A Novel Chemodosimeter for Fluoride Ions. *Tetrahedron Lett.* **2011**, *52*, 1313-1316; DOI: 10.1016/j.tetlet.2011.01.057.

[19] Padié, C.; Zeitler, K. A Novel Reaction-Based, Chromogenic and "Turn-on" Fluorescent Chemodosimeter for Fluoride Detection. *New J. Chem.* **2011**, *35*, 994-997; DOI: 10.1039/c0nj00937g.

[20] Hu, J.; Li, C.; Cui, Y.; Liu, S. Highly Selective Colorimetric and Fluorometric Probes for Fluoride Ions Based on Nitrobenzofurazan-Containing Polymers. *Macromol. Rapid Commun.* **2011**, *32*, 610-615; DOI: 10.1002/marc.201100024.

[21] Liu, J.; Yang, X.; Wang, K.; Yang, R.; Ji, H.; Yang, L.; Wu, C. A Switchable Fluorescent Quantum Dot Probe Based on Aggregation/Disaggregation Mechanism. *Chem. Commun.* **2011**, *47*, 935-937; DOI: 10.1039/c0cc03993d.

[22] Kim, E.; Kim, H. J.; Bae, D. R.; Lee, S. J.; Cho, E. J.; Seo, M. R.; Kim, J. S.; Jung, J. H. Selective Fluoride Sensing Using Organic-Inorganic Hybrid Nanomaterials Containing Anthraquinone. *New J. Chem.* **2008**, *32*, 1003-1007; DOI: 10.1039/b714406g.

[23] Mulrooney, R. C.; Singh, N.; Kaur, N.; Callan, J. F. An "Off-On" Sensor for Fluoride Using Luminescent CdSe/ZnS Quantum Dots. *Chem. Commun.* **2009**, 686-688; DOI: 10.1039/b817569a.